Suppression of *Plasmodium* MIF-CD74 Signaling Protects Against Severe Malaria

Alvaro Baeza Garcia[1*], Edwin Siu[1], Xin Du[1], Lin Leng[1], Blandine Franke-Fayard[3], Chris J Janse[3], Shanshan W Howland[4], Laurent Rénia[4], Elias Lolis[5], Richard Bucala[1,2*]

Affiliations:

[1]Departments of Internal Medicine, [2]Pharmacology, Yale School of Medicine, and [2]Epidemiology of Microbial Diseases, Yale School of Public Health, New Haven, Connecticut 06520, USA.[3] Department of Parasitology, Leiden University Medical Center, Leiden, Netherlands, [4]Singapore Immunology Network, Agency for Science, Technology and Research (A*STAR), Singapore, Singapore. [5] Department of Pharmacology, School of Medicine, Yale University, New Haven, CT, 06510, USA.

*Correspondence to Richard Bucala, Department of Internal Medicine, Yale University School of Medicine P.O. Box 208031, 300 Cedar St., New Haven, Connecticut 06520-8031, USA. Telephone at (203) 785-2453. Fax at (203) 785-5415. Email at richard.bucala@yale.edu

*Correspondence to Alvaro Baeza Garcia. Email at alvaro.baeza-garcia@inserm.fr

Abstract

Malaria begins when mosquito-borne *Plasmodium* sporozoites invade hepatocytes and usurp host pathways to support the differentiation and multiplication of erythrocyte-infective, merozoite progeny. All *Plasmodium* species encode an orthologue of the innate cytokine, Macrophage Migration Inhibitory Factor (MIF), which functions in mammalian biology to regulate innate responses. Using a genetically-targeted strain of *Plasmodium berghei*, we demonstrate that the *Plasmodium* MIF orthologue, PMIF, activates the cognate host MIF receptor, CD74, to inhibit the host-protective apoptosis response of infected hepatocytes and sustain *Plasmodium* development and replication. Infection of CD74 deficient (*Cd74*$^{-/-}$) mice revealed a significantly reduced liver burden of *Plasmodium* parasites compared with WT mice and protection from experimental cerebral malaria (ECM) development. Protection from ECM additionally was associated with the inability of *Cd74*$^{-/-}$ brain microvessel endothelial cells to present parasite antigen to sequestered, *Plasmodium*-specific CD8^{+} T cells. A novel pharmacologic PMIF-selective antagonist reduced PMIF/CD74 signaling and liver-stage parasite burden, and fully protected mice from ECM. These findings reveal a conserved mechanism for *Plasmodium* usurpation of host CD74 signaling and suggest a tractable approach for new pharmacologic intervention.

Introduction

Malaria caused by parasites of the genus *Plasmodium* is the most deadly parasitic disease, causing approximately half a million deaths annually [1]. *Plasmodium* sporozoites enter the skin through the bite of infected *Anopheles* mosquitoes and transit through the bloodstream to invade the liver, where a single infected hepatocyte produces tens of thousands of erythrocyte-infectious merozoites and initiates the erythrocytic cycle of infection. During the pre-erythrocytic stage, *Plasmodium*-infected hepatocytes are re-programmed toward metabolic pathways essential for parasite differentiation and proliferation and become resistant to apoptosis, which is a host-protective mechanism to restrict infection. Prior studies of *Plasmodium*-infected cells have implicated pro-survival roles for hepatocyte growth factor signaling [2, 3] and inhibition of the tumor suppressor p53, activated by cellular stress to initiate programmed cell death [4]. The subsequent erythrocytic stage of infection produces the disease's clinical manifestations [5], including the most severe complication of *P. falciparum* infection: cerebral malaria leading to impaired consciousness, seizures, coma, and subsequent mortality [6]. The experimental cerebral malaria (ECM) animal model by infection of susceptible C57BL/6J mice with *Plasmodium berghei* ANKA (*Pb*A) reproduces many neurological signs and pathologic changes associated with human cerebral malaria. ECM is triggered by parasitized erythrocytes in the cerebral microvasculature leading to the production of inflammatory molecules such as IFN-γ, granzyme B, and perforin, and is associated with the recruitment and accumulation of effector CD8+ T cells [7, 8].

Both host and parasite factors contribute to the pre- and erythrocytic stages of infection and severe malaria development. *Plasmodium* parasites express intricate strategies to evade immune detection and destruction. It is noteworthy that all *Plasmodium* species analyzed genetically encode an orthologue of the mammalian cytokine macrophage migration inhibitory factor (MIF) [9, 10]. MIF sustains activation responses by promoting innate cell survival, which occurs by signaling through its cognate receptor CD74, leading to sustained ERK1/2 activation and reducing cellular p53 activity [11, 12 , 13]. *Plasmodium* MIF (PMIF) is highly conserved in all known *Plasmodium* genomes; for instance, only a single amino acid distinguishes murine *Plasmodium berghei* from human *P. falciparum* PMIF [9, 10]. Recent evidence has implicated PMIF in the growth and development of liver-stage parasites [14, 15], and PMIF binds with high affinity to the host receptor CD74 [16, 17], which has been independently identified as a susceptibility factor for murine *Plasmodium* infection [18].

In the present study, we show that PMIF has a central role in *Plasmodium* liver replication and cerebral malaria onset. Mechanistically, PMIF activates the hepatocellular MIF host receptor CD74 to inhibit the apoptosis of infected hepatocytes, thus promoting *Plasmodium* development and replication. Mice infected with *Pb*A*mif*- sporozoites or *Pb*AWT infected *Cd74-/-* mice are resistant to cerebral malaria. Cerebral malaria onset further relies on the contribution of endothelial cell CD74, which is upregulated in the brains of infected mice, to promote parasite antigen presentation to brain sequestered *Plasmodium*-specific $CD8^+$ T cells. Pharmacologic inhibition of the PMIF/CD74 interaction by the PMIF-selective, small molecule antagonist 26k reduces the survival of infected cells, decreases liver-stage parasite burden, and fully protects mice from acute cerebral malaria.

Results

PMIF promotes survival of *Plasmodium*-infected hepatocytes by inhibiting p53 activity and contributes to the development of ECM.

P. berghei ANKA parasites that are genetically deficient in PMIF (*Pb*A*mif*-) develop normally in their mosquito hosts as well as during blood-stage infection [16]. However, we observed that parasite burden was reduced in HepG2 hepatocytes infected with *Pb*A*mif*- sporozoites compared with wild-type *Pb*A (*Pb*AWT) sporozoites (**Figure 1A**). Examination of circumsporozoite (CSP) and merozoite surface protein-1 (MSP-1) as indicators of parasite maturation [19] showed that while CSP was expressed in similar levels, there was reduced expression of MSP-1 in the *Pb*A*mif*- HepG2 infected cells, suggesting that PMIF is not necessary for hepatocyte infection but may have a permissive role in pre-erythrocytic parasite development (**Figure 1B, with S1A** showing *Pb*AHSP70 as a loading control for *Pb*AMSP-1). Mammalian MIF has been shown to promote monocyte survival by increasing phosphorylation of the pro-apoptotic protein p53 at Ser^{15} [11, 13]. We treated infected HepG2 cells with the nitric oxide (NO) donor sodium nitroprusside (SNP) to induce p53 accumulation and apoptosis. We found that HepG2 cells infected with *Pb*A*mif*- sporozoites were significantly more susceptible to NO-induced apoptosis than cells cultured with *Pb*AWT parasites despite a reduced infection level when compared with *Pb*AWT sporozoites **(Figure 1C**). The protection from apoptosis observed in *Pb*AWT infected HepG2 cells was associated with decreased phospho-$p53^{Ser15}$ and intracellular p53 content when compared with *Pb*A*mif*- infected cells (**Figure 1D)** [20, 21]. Induction of apoptosis in *Pb*A*mif*- versus *Pb*AWT infected cells also was associated with increased Akt phosphorylation (**Figure S1B**).

We confirmed these *in vitro* findings by infecting mice with *Pb*AWT or *Pb*A*mif*- sporozoites. The livers of *Pb*A*mif*- infected mice showed an 80% reduction in parasite burden compared with the livers of *Pb*AWT infected mice, and this was associated with an attendant decrease in expression of the pro-survival gene *Bcl-2* and an increase in the expression of the pro-apoptotic gene *Bad* **(Figure S1C**). We next examined the contribution of PMIF to the development of cerebral malaria. Mice infected with *Pb*AWT sporozoites showed neurological symptoms and mortality within 8-9 days after infection, while mice infected with *Pb*A*mif*- sporozoites didn't exhibit signs of ECM and survived until day 25 after infection (**Figure S1D**). When mice were infected with *Pb*AWT or *Pb*A*mif*- iRBC, there was no difference in ECM manifestations, and all the mice succumbed by day seven after infection (**Figure S1F**). Our results show that PMIF antagonizes hepatocyte apoptotic pathways and promotes initial sporozoite infection in ECM development.

PMIF action is mediated by the host MIF receptor CD74 to promote *Plasmodium*-infected hepatocyte survival and p53 inhibition.

We confirmed the role of PMIF in signaling through the host MIF receptor by studying sporozoite infection in HepG2 cells after knockdown of CD74. Hepatocytes treated with shCD74 to reduce CD74 expression had decreased parasite burden compared with treatment with a non-relevant shRNA (shCon) (**Figure 2A** and **S1G** for the viability of HepG2 cells before infection). As expected, *Pb*AWT infected shCD74-treated cells were more susceptible to apoptosis than shCon-treated cells (**Figure 2B**). Apoptosis induction also was associated with increased cellular $p53^{Ser15}$ and p53 accumulation in the infected HepG2 cells with reduced CD74 expression (**Figure 2C**). Infection of mice genetically deficient in the cognate host MIF receptor CD74 ($Cd74^{-/-}$) with *Pb*AWT sporozoites revealed a significantly reduced liver burden of *Plasmodium* parasites than in WT ($Cd74^{+/+}$) mice (**Figure 2D**), which was associated with a delay in blood-stage patency from 2 to 6 days post-infection (**Figure 2E**). These results support the essential role of CD74 in mediating PMIF action and in promoting *Plasmodium* pre-erythrocytic development leading to blood-stage infection.

CD74 is overexpressed in the brain of *Pb*AWT infected mice and contributes to ECM development.

The marked effect of CD74 on the development of *Pb*AWT parasites in the liver and the progression of blood-stage infection prompted us to examine the potential role of CD74 in

the pathogenesis of ECM. We measured the expression of CD74 in *Pb*AWT-infected mouse brains during ECM and observed an increase in *Cd74* mRNA expression compared with uninfected mice (**Figure 3A**).

We next challenged WT and *Cd74*$^{-/-}$ mice with *Pb*AWT iRBCs and assessed ECM development. While 100% of the WT mice exhibited neurological symptoms within 7-8 days after infection, the *Cd74*$^{-/-}$ mice were fully protected from ECM and succumbed to hyperparasitemia by day 30 after infection (**Figure 3B,C and S2A**). We found no significant differences in parasitemia between *Pb*AWT-infected WT or *Cd74*$^{-/-}$ mice during the asymptomatic blood-stage, suggesting that *Cd74* deficiency does not affect parasite replication in the erythrocyte (**Figure S2B**). The same results were observed in *Cd74*$^{-/-}$ mice infected with *Pb*A*mif-* parasites (**Figures S2C, D and E**). The protection of *Cd74*$^{-/-}$ mice was associated with the downregulation of IFN-γ, perforin, and granzyme B expression in the brains of *Cd74*$^{-/-}$ versus WT mice but without an appreciable difference in the quantity of brain sequestered parasites (**Figure 3D and Figure S2F**). To evaluate the contribution of the PMIF/CD74 interaction to the development of ECM, we infected WT mice with *Pb*AWT or *Pb*A*mif-* sporozoites. We measured the expression of CD74 in the brain of infected mice during ECM and observed an increase in *Cd74* mRNA expression in *Pb*AWT infected mice compared with brains of *Pb*A*mif-* infected mice (**Figure S2G**). Additionally, the expression of the inflammatory molecules IFN-γ, perforin, and granzyme B increased in the brain of mice infected with *Pb*AWT parasites (**Figure S2H**). $CD8^+$ T cells are essential for the development of ECM and contribute directly to ECM pathology [22]. Thus, we investigated if $CD8^+$ T cells from *Cd74*$^{-/-}$ mice have an impaired response to *Pb*A infection. We measured the amount of brain sequestered $CD8^+$ T cells responding to *Pb*A by using a T cell receptor tetramer specific to the *Pb*AGAP50 antigen [23]. Notably, the amount of brain-sequestered *Pb*AGAP50-specific $CD8^+$ T cells was not significantly different between WT and *Cd74*$^{-/-}$ mice (**Figure 3E**), indicating that *Cd74*$^{-/-}$ mice can mount a *Pb*AWT responsive $CD8^+$ T cells response in the brain. Nevertheless, in *Cd74*$^{-/-}$ mice, CD8 T cell effector functions were strongly suppressed, as indicated by the reduced frequency of *Pb*GAP50-specific $CD8^+$ T cells expressing the ECM associated inflammatory molecule granzyme B (**Figure 3F**). Our findings suggest that *Pb*AWT responsive $CD8^+$ T cells from *Cd74*$^{-/-}$ *mice* undergo priming and trafficking to the brain during *Pb*AWT blood-stage infection, but do not express the inflammatory effector response associated with the development of ECM.

Brain vascular endothelium becomes activated during malaria infection with the ability to process and cross-present *Plasmodium* antigens [23], and contribute to the T cell effector

response and inflammation that underlies ECM [22]. In addition to CD74's role as the cognate MIF receptor [12], it functions intracellularly as the MHC class II invariant chain [24] and it has been implicated in an MHC class I cross-presentation pathway for cytolytic T lymphocytes (CTL) [25]. We hypothesized that CD74 expressed by activated brain endothelium may cross-present *Pb*A antigens to prime infiltrating CD8+T cells. Accordingly, we assessed the ability of *Pb*A antigen-pulsed, brain-derived endothelial to activate T cells by employing the LR-BSL8.4a reporter T cell line that expresses LacZ in response to the *Pb*A-GAP50 epitope [8]. *Cd74*$^{-/-}$ brain-derived endothelial cells were less able to activate LR-BSL8.4a T cells in the presence of *Pb*A antigens when compared to WT brain-derived endothelial cells (**Figure 3G**). We confirmed these results by isolating brain microvessels from *Pb*AWT infected WT and *Cd74*$^{-/-}$ mice at the time of ECM development and incubating them with LR-BSL8.4a reporter T cells for measurement of LacZ expression. Microvessels from *Pb*A-infected WT mice showed a greater ability to cross-present *Pb*A antigens than microvessels from *Cd74*$^{-/-}$ mice (**Figure 3H**). These results suggest a specific role for brain endothelial CD74 in the presentation of *Pb*A antigens to CD8+ T cells. Because *Cd74* expression in the brain is upregulated by PMIF (**Figure S2G)** we next tested if PMIF also has a role in the cross-presentation of *Plasmodium* antigens mediated by CD74. We isolated brain microvessels from mice infected with *Pb*AWT or *Pb*A*mif*- sporozoites at the time of ECM onset and incubated them with LR-BSL8.4a reporter T cells. We observed that microvessels from mice infected with *Pb*AWT parasites exhibited a greater ability to cross-present *Pb*A antigen than microvessels from *Pb*A*mif*- infected mice (**Figure S2I)**.

We examined if a dysfunctional cytotoxic response in CD74 deficient CD8$^+$ T cells reduced ECM symptoms. For this we adoptively transferred WT or *Cd74*$^{-/-}$ CD8$^+$ T cells, into naïve *Cd8*$^{-/-}$ or *Cd8*$^{-/-}$*Cd74*$^{-/-}$ recipient mice by infection with *Pb*A iRBCs three days later. Recipient *Cd8*$^{-/-}$ mice that received WT or *Cd74*$^{-/-}$ CD8$^+$ T cells from *Pb*A infected mice showed signs of ECM and succumbed by day 10, whereas recipient *Cd8*$^{-/-}$ *Cd74*$^{-/-}$ mice receiving WT or *Cd74*$^{-/-}$ CD8$^+$ T cells from *Pb*A infected mice did not show ECM symptoms and succumbed by 20 days after infection (**Figure S2J**). We next assessed cross-presentation of *Pb*A antigens *ex vivo* by using brain microvessels from *Cd8*$^{-/-}$ and *Cd8*$^{-/-}$*Cd74*$^{-/-}$ mice infected with *Pb*A after adoptive transfer with CD8$^+$ T cells from WT or *Cd74*$^{-/-}$ mice. Only *Cd8*$^{-/-}$ mice that received *Cd8*$^+$ or *Cd8*$^{-/-}$*Cd74*$^{-/-}$ T cells cross-present *Pb*A antigens (**Figure S2K**). Together these results indicate that CD74 expression by brain endothelial cells contributes to cross-presentation of *Pb*A to CD8$^+$ T cells and ECM development.

Finally, we assessed the potential clinical significance of anti-PMIF antibodies, which circulate in malaria patients [26], by measuring their ability to interfere with PMIF binding to CD74 *in vitro*. Using an established ELISA-based binding assay [27, 28], we observed that such sera inhibited PMIF binding to the recombinant CD74 ectodomain when compared to sera from uninfected healthy controls, and moreover, that sera from patients with clinically uncomplicated malaria were more effective in reducing PMIF/CD74 interaction than sera from patients with complicated malaria (*e.g.,* severe anemia, cerebral malaria [17]) (**Figure S2L**). These data suggest a possible role for an anti-PMIF antibody response in clinical sequelae that warrants further investigation.

Pharmacologic PMIF antagonism reduces *Pb*A infection and protects against cerebral malaria.

Our experimental results support a central role for CD74 and its activation by PMIF in malaria infection by promoting parasite liver replication, blood-stage infection, and subsequent ECM pathophysiology. Small molecule MIF inhibitors have been developed and are in clinical evaluation [29, 30]. We recently identified a small molecule PMIF antagonist, termed 26k, with low selectivity for host MIF (K_i = 40 nM for PMIF versus Ki >100 μM for MIF) [31] that blocks PMIF interaction with the CD74 ectodomain [28] and downstream ERK1/2 MAPK signaling (**Figure S3A**). We treated *Pb*A sporozoite infected hepatocytes with 26k *in vitro* and measured parasite burden by expression of *Pb*A18s RNA together with sensitivity to apoptosis induction. Parasite burden decreased in the cells treated with 26k compared with vehicle (**Figure 4A**). Hepatocytes infected with *Pb*A and treated with 26k also were more susceptible to apoptosis as evidenced by Annexin V staining. Moreover, treated cells showed increased p53 phosphorylation and intracellular accumulation, a known consequence of CD74 blockade [11] (**Figure 4B, C**).

To determine if these results could be translated *in vivo*, we treated C57BL/6J mice with 26k before infection with $2x10^3$ *Pb*A sporozoites and then once daily for 2 days. Liver-stage infection, blood-stage patency, and the development of cerebral malaria and lethality were assessed. Treatment with three doses of 26k (0, 24, 48 h) dramatically decreased parasite burden in the liver at 48 h after infection compared with vehicle controls (**Figure 4D, E**). Sporozoite infection, in turn, led to blood-stage patency after 3 days in vehicle-treated mice but not until day 5 in the 26k treated group (**Figure S3B**). All vehicle-treated mice developed ECM symptoms (head deviation, ataxia, and paraplegia) 8 days after sporozoite infection, and

all mice succumbed to cerebral malaria by days 9-10. By contrast, all mice treated with 26k were spared from cerebral malaria symptoms and did not succumb until day 30 (**Figure 4F)**.

We also examined the impact of 26k on *Plasmodium* antigen cross-presentation by brain microvascular endothelial cells. Brain microvessels from *P*bA infected WT mice were isolated at the time of ECM and treated *in vitro* with 26k (or vehicle) together with LR-BSL8.4a reporter T cells. LacZ expression was then measured after overnight incubation. Only microvessels from *Pb*A-infected mice treated with vehicle were able to cross-present *Pb*A antigen and induce LacZ expression (**Figure 4G**). We also examined if 26k administration prevented ECM when mice were inoculated directly with *Pb*A-infected erythrocytes. We observed only partial protection from ECM in mice treated with 26k in this model (**Figure S3C**), suggesting that the dominant effect of 26k is on liver-stage *Pb*A development. Taken together, these results support the conclusion that pharmacologic inhibition of the PMIF/CD74 interaction may be a promising approach to protect from liver infection and ECM.

Discussion

Plasmodium parasites have evolved highly specialized strategies for host invasion, evading immune destruction, and sustaining infection to ensure their life cycle completion. Our study highlights the importance of the pre-erythrocytic phase of malaria infection as an essential stage in the development of host immune responses and the subsequent progression of ECM. This has important implications for the investigation of *Plasmodium* genes whose pathologic relevance may be underestimated based on the route of the infection.

Our data indicate that PMIF, which appears to be universally expressed by the *Plasmodium* genus [30, 31], and its interaction with hepatocyte CD74 is an adaptive mechanism for sporozoites to usurp a host-protective apoptosis pathway in order to prevent their destruction and enable parasite differentiation and patent infection. PMIF appears to impact *Plasmodium* liver development without influencing its infectivity of host hepatocytes [14, 15]. Moreover, inhibition of PMIF activity by vaccination is associated with a higher frequency of memory liver resident CD8+ T cells [15]. Complementary genetic studies also indicate that relative increases in liver CD74 expression correlate with susceptibility to successful host hepatocyte infection [18]. Immunostaining studies suggest that PMIF is expressed on the surface of infective sporozoites and within the parasitophorous vacuole during the liver stage development [14, 16]. The precise localization of PMIF interaction with host CD74 is currently unclear; however, we suggest two possible scenarios. The first is by contact between PMIF on the invading sporozoite and CD74 expressed on the hepatocyte cell surface,

leading to the activation of Akt and cellular pro-survival pathways [4]. The second is after sporozoite internalization and contact between PMIF in the parasitophorous vacuole and endosomal-expressed CD74 during later-stage *Plasmodium* development [32].

PMIF additionally promotes the expression of CD74 in the brain of infected mice, and our data support a distinct and previously unforeseen role in the cross-presentation of *Plasmodium* antigens to promote a CD8+ T cell-mediated, pathologic inflammatory response. Prior studies have reported that IFNγ enhances cell surface expression of CD74 [33], and during cerebral malaria, the expression of IFNγ increases in the brain [34], contributing to the induction of CD74 expression in EC. While dendritic cells are considered the major antigen-presenting cells responsible for activating CD4 and CD8 T cell responses against *Plasmodium* [35], endothelial cells are major contributors to blood-brain barrier breakdown and neurological disease, and also contribute in this respect [8, 23]. Our data suggest that CD74 promotes the cross-presentation of *Plasmodium* antigen by brain EC to promote ECM development,

We additionally show that the PMIF/CD74 interaction pathway is amenable to pharmacologic targeting. The PMIF selective antagonist 26k [28,29] recapitulates the effect observed by the absence of PMIF or its host receptor *Cd74*. 26k reduces *Plasmodium* intrahepatic development and provides full protection against cerebral malaria in the *Pb*A model of disease. These results, together with precedent co-crystallization studies supporting the selectivity of 26k for PMIF versus host MIF, provide proof-of-concept for pharmacologic PMIF antagonism as a tractable approach for both malaria prophylaxis and liver-stage treatment, and potentially across a range of *Plasmodium* species and strains [29]. PMIF is extremely conserved among *Plasmodium* species, with only 5 single nucleotide polymorphisms in PMIF among the 202 sequenced strains of *P. falciparum* present in the PlasmoDB resource [9, 10]. This high degree of structural conservation may be auspicious for therapeutic targeting, particularly in a genomically complex pathogen prone to resistance development. Additional studies to optimize the absorption, distribution, metabolism and excretion properties of 26k will be necessary to advance PMIF selective inhibitors such as 26K into clinical development.

Materials and Methods

Mice

Female WT or *Cd74*$^{-/-}$ C57BL/6J mice between 6-10 weeks of age were purchased from The Jackson Laboratory and used for study. *Cd8*$^{-/-}$*Cd74*$^{-/-}$ mice were obtained by crossing *Cd8*$^{-/-}$ with *Cd74*$^{-/-}$ mice. Swiss Webster mice were obtained from The Jackson Laboratory. All animals were maintained in specific pathogen-free facility at Yale Animal Resource Center. All animal procedures followed federal guidelines and were approved by the Yale University Animal Care and Use Committee, approval number 2017-10929.

Parasites and infection

*Pb*AWT (MR4), *Pb*A*mif*- (Leiden Malaria Group) [16] or *Pb*AWT-GFP-luciferase (MR4) parasites were cycled between Swiss Webster mice and *Anopheles stephensi* mosquitoes. For erythrocytic infection, cryopreserved stocks of infected red blood cells (iRBCs) were injected (10^6 iRBCs/mouse) and blood parasitemia was monitored by Giemsa-stained blood smears and flow cytometry [15]. For the pre-erythrocytic stage infection, salivary gland sporozoites were extracted from infected mosquitoes on day 19 post-blood meal infection. WT or *Cd74*$^{-/-}$ C57BL/6J mice were infected by i.v. tail injection of 2000 *Pb*AWT, *Pb*A*mif*- or *Pb*AWT-GFP-luciferase sporozoites, and blood patency was monitored beginning day 3 by blood smear and flow cytometry. Liver parasite burden was monitored at 48 h after infection using an IVIS imaging system (Caliper) or quantitative PCR [15].

For adoptive transfer, splenocytes were isolated six days after infection of WT or *Cd74-/-* mice infected with 10^6 *Pb*AWT iRBC, CD8 T cells were purified with anti-CD8 (Ly-2, Miltenyi Biotech) according to the manufacturer's protocol. $1x10^7$ cells were transferred i.v. into recipient C57BL6/J *Cd8*$^{-/-}$ or *Cd8*$^{-/-}$*Cd74*$^{-/-}$ mice, and mice infected three days after with 10^6 *Pb*AWT iRBC.

Hepatocyte infection, apoptosis induction, Annexin V assay and quantification of p53 by western blotting

For apoptosis assessment, 1×10^5 HepG2 cells (ATCC) were seeded in complete EMEM medium (ATCC) (10% FBS (Atlanta Biologicals), 1% streptomycin/penicillin (Thermo-Fisher), and infected with 2 $x10^3$ *P*bAWT or *Pb*A*mif*- sporozoites. 48 h after infection, cells were treated with 1 mM of SNP (Sodium Nitroprusside, Sigma) for 4 h or left untreated as a control. For PMIF pharmacologic inhibition, cells were treated with 26k (10 nM, 100 nM) or with an equivalent concentration of vehicle (0.1% DMSO) (Sigma) before infection. Cells then

were detached with Acutase (MP Bio) and cell suspensions split for Western blot or Annexin V analysis. For Annexin V analyses, cells were stained with Pacific Blue-Annexin V and 7AAD (7-aminoactinomycin D) (Biolegend) before running in a LSRII cytometer (BD Biosciences). For quantification of p53 by western blotting, *Pb*AWT-infected HepG2 hepatocytes were detached with Accutase (MP biolabs) and pelleted. Western blots were performed by lysing cell pellets in RIPA buffer (ThermoFisher) according to standard protocols and using antibodies directed against p53-Ser^{15} (clone 1C12) or total p53 (pAb) (Cell Signaling Technology). For quantification, density signals were normalized to an anti-β-actin Ab (LICOR) and developed with anti-mouse or anti-rabbit Abs conjugated with HRP (LI-COR Biosciences). Membranes were visualized using an Odyssey-Fc imaging system (LI-COR Biosciences). Each western blot panel was developed from the same membrane that was re-probed after stripping.

Quantification of liver-stage *Pb*AWT and *Pb*Amif- infection, and *Cd74* knockdown

HepG2 liver cells infected with *Pb*AWT or *Pb*A*mif*- sporozoites were lysed at 24 h or 48 h after infection, cellular proteins transferred to PVDF membranes (Millipore), and analyzed by western blotting using anti-CSP (MRA-100) and anti-MSP-1 (MRA-667) antibodies obtained from MR4 ATCC (Manassas, VA). β-actin was used as loading control. For treatment with siRNA, hepatocytes were transfected with 15 pmol of siRNA (Ambion) targeting CD74 mRNA (3 target sequences in exon 2) or siCtrl (scrambled unrelated sequence) as a negative control. siRNA was complexed with Lipofectamine RNAimax reagent (ThermoFisher) and added to the cells for 24 h; cells then were infected with *Pb*AWT sporozoites.

Murine *Pb*A infection and 26k treatment

C57BL/6J mice received three i.p. injections of 26k (4-(3-methoxy-5-methylphenoxy)-2-(4-methoxyphenyl)-6-methylpyridine) [31], synthesized by CheminPharma LLC (Branford, Connecticut), at 80 mg/kg after dissolution in PEG400 (Sigma-Aldrich) in a sonicating water bath. HP-P-cyclodextrin (Sigma-Aldrich) was added to prepare a 4 mg/ml solution. Control mice received vehicle alone. Immediately after the first i.p. injection, mice were infected i.v. with 2×10^3 *Pb*A-luc-GFP sporozoites; the second and third injections of 26k were given 24 h and 48 h later, and always after measurement of *Pb*A liver burden. The *Pb*A liver burden was quantified 48 h after infection by luminescence emission after luciferin injection (Perkin Elmer) using an IVIS apparatus (Caliper). Livers were excised 48 h after infection, the total RNA extracted and purified with Trizol (Life Technologies), and parasites quantified by RT-qPCR using primers for *Pb*18s.

Brain microvessel cross-presentation assay

WT, *Cd74*$^{-/-}$, *Cd8*$^{-/-}$ or *Cd8*$^{-/-}$*Cd74*$^{-/-}$ C57BL/6J mice were infected by intravenous injection of sporozoites or by intraperitoneal injection of *Pb*A infected red blood cells. Infected mice were sacrificed when the signs of ECM (head deviation, ataxia) were manifested. Control naïve mice were sacrificed contemporaneously with the experimental group. The technique for isolating brain microvessels and quantification of cross-presentation of the parasite-derived GAP50 epitope by LR-BSL8.4a reporter T cells [23] was performed according to the published protocol [22]. Quantification of β-galactosidase activity by activated LR-BSL8.4a reporter cells was performed by using a luminescence β-galactosidase assay (ThermoFisher) and the resultant signal quantified with a microplate reader (Tecan).

Isolation of Brain-infiltrating lymphocytes for flow cytometry.

Naïve or infected WT and C*d74*$^{-/-}$ C57BL/6J mice were sacrificed and perfused intra-cardially with 20 ml 1x DPBS (' 'Dulbecco's Phosphate Buffer Saline). Brains were minced in RPMI, digested with 10 µg/ml of DNase I (Sigma) and 0.5 mg/ml for 30 min at 37ºC, and homogenized with a pestle then filtered with a 70 µm cell-strainer (BD Falcon). The suspension then was centrifuged at 200xg for 5min, and the pellet resuspended in 90% Percoll (GE Healthcare) and overlaid with a 70%, 50% and 30% Percoll gradient. After centrifugation at 500xg for 10 min, the cell interphase was collected treated with RBC lysis buffer, washed once, and resuspended in complete RPMI medium (containing 10% FBS (Atlanta Biologicals) and 1% penicillin-streptomycin (Thermo Fisher)). 100 µl of brain cell suspensions were stimulated with 1 µM of peptide (SQLLNAKYL) in the presence of 10 µg/ml Brefeldin A. After 5 h incubation at 37°C, the cells were centrifuged and washed once with 100 µl DPBS + 5% FBS. The cells then were re-suspended and incubated with FITC-labelled SQLLNAKYL-H-^{2b} tetramer for 15 min on ice before staining with anti-CD8-PE Cy7 (clone 53-6.7, Biolegend), anti-CD4-PerCP Cy 5.5 (clone RM4, Biolegend) and anti-CD11a antibodies in the presence of FCR-block for 20 min on ice. Cells were washed, pelleted and permeabilized by re-suspension in 100 µl Fix/Perm buffer on ice for 15 min. Cells then were washed once with 1x Perm Wash buffer (BD Bioscience), and stained with anti-IFN-γ-APC-Cy7 (clone XMG1.2, Biolegend), and GrmzB-Pe-Cy7 (clone NGZB,eBioescience) in 1x Perm Wash buffer (BD Bioesciences) for 20 min on ice. Finally, cells were washed, centrifuged once, and re-suspended in 200 µl PBS+5% FBS for flow cytometry. The data were acquired on a LSRII flow cytometer (BD Biosciences) and analyzed using the FlowJo software (version 10).

Patient Samples and PMIF-CD74 binding assay

Sera from a Zambian cohort of *P.falciparum*-infected patients were used in the study [17, 36]. The interaction between PMIF and CD74 was analyzed as previously described [27, 28]. Briefly, 96-well plate were coated with 26 ng/ml of recombinant CD74 ectodomain (aa 114-243) in PBS and incubated overnight at 4°C. After washing with PBS/0.1% Tween-20, the plate was blocked with Superblock reagent (Pierce) for 2 hours. Biotinylated recombinant PMIF (5ng/ml) was incubated for 45 min, with human serum (diluted 1:1000) from a previously described repository of healthy donors or subjects with uncomplicated or complicated malaria [17]. After washing and incubation with Streptavidin-HRP (Roche), the peroxidase substrate 3,3'-5,5'-tetramethylbenzidine (TMB, Roche) was added and after 20 min incubation the reaction was stopped with 1N H_2SO_4/HCl. The results were expressed as the percentage of binding in the presence versus the absence of serum.

Statistical analysis

All statistical analysis was performed as described before (15), using Software Prism v.6.0, (GraphPad). Statistical significance was indicated at p values of less than 0.05, 0.01, or 0.001. All data were expressed as a mean ± SD of at least two independent experiments. Mouse survival times were analyzed by the Mantel-Cox log-rank test. All other data were first tested for Gaussian distribution of values using a D'Agostino-Pearson normality test. The statistical significance of differences was assessed using the Kruskal-Wallis or Mann–Whitney U test for non-parametric data distribution and ANOVA or Student's t-test for parametric data.

Ethics Approval

All animal procedures followed federal guidelines and were approved by the Yale University Animal Care and Use Committee, approval number 2017-10929. De-identified human sera collected from a prior study were used for in vitro ELISA studies (Yale HIC #0804003730).

Figures Legends

Figure 1. PMIF influences *Pb*A liver-stage development and promotes survival of *Plasmodium*-infected hepatocytes by inhibiting p53 activity. $1x10^5$ hepatocytes (HepG2 cells) were infected with $2x10^3$ *Pb*AWT or *Pb*A*mif*- sporozoites. **A**, Parasite load was measured by quantitative PCR of *Pb*A 18S rRNA relative to host GAPDH 48 h after infection. Data are from three independent experiments performed in duplicate. Bars represent the mean ± SD; *p=0.0286 by Mann–Whitney test. **B**, Hepatocellular content of CSP and MSP-1 at 24 h and 48 h after infection with $2x10^3$ *Pb*AWT or *Pb*A*mif*- sporozoites assessed by western blot relative to *β*-actin as loading control. $1x10^5$ *Pb*AWT or *Pb*A*mif*- infected hepatocytes were cultured for 48 h and treated with 1 mM of the NO donor sodium nitroprusside (SNP) for 4 h to induce apoptosis. **C,** Percentage of apoptotic cells measured by AnnexinV and 7AAD (7-amino-actinomycin D) staining. Data are from three independent experiments performed in duplicate. Bars represent the mean ± SD; *p=0.0133; **p=0.0011; $^{\Psi}$p<0.0001; by Kruskal-Wallis test. **D,** Lysates of the same hepatocytes in C were assessed for total p53 and $p53^{Ser15}$ by Western blotting. NI: non-infected. Numerals represent the mean densitometric scanning ratios. Data are representative of two independent replicates experiments for the western blot analysis.

Figure 2. The host MIF receptor CD74 mediates PMIF action in promoting *Plasmodium*-infected hepatocyte survival and p53 inhibition. Cultured hepatocytes ($1x10^5$ HepG2 cells) were treated with 10 nM of shRNA directed at CD74 (shCD74) or a control shRNA (shCon), and infected 24 h later with $2x10^3$ *Pb*AWT sporozoites. **A**. *Cd74* mRNA expression measured by qPCR in HepG2 after 48h treatment. Data are from three independent experiments performed in duplicate. Bars represent the mean ± SD; **p= 0.002 by Mann-Whitney test. **B**, Parasite load was measured by quantitative PCR of *Pb*A 18S rRNA relative to host GAPDH. $1x10^5$ *Pb*AWT infected hepatocytes cultured for 48 h were treated with 1 mM of the NO donor SNP for 4 h to induce apoptosis. Data are from three independent experiments performed in duplicate. Bars represent the mean ± SD; **p=0.002 by Mann–Whitney test. **C,** Percentage of apoptotic cells measured by AnnexinV and 7AAD staining in *Pb*AWT infected HepG2 cells treated with shCon or shCD74. Numerals represent the densitometric scanning ratios. Data are from three independent experiments performed in duplicate. Bars represent the mean ± SD; **p=0.0095 and n.s.=non-significant; by Kruskal-Wallis test. **D,** Lysates of the same hepatocytes as in B were assessed for total p53 and $p53^{Ser15}$ by Western blotting with β-actin as loading control. NI: non-infected, INF: *Pb*AWT infected. Numerals represent the mean

densitometric scanning ratios. Data are representative of two independent replicate experiments for the western blot analysis. **E**, Wild type (WT) or *Cd74*$^{-/-}$ C57BL/6J mice were infected i.v. with 2x10^3 *Pb*A-luciferase sporozoites and liver *Pb*A-luc load quantified by luminescence at 48 h after infection. Bars represent the mean ± SD; **p=0.0022; by Mann-Whitney test. **F**, Kaplan-Meier plots showing the percentage of WT (●) and *Cd74-/-* (○) C57BL/6J mice with blood-stage patency following i.v. infection with 2x10^3 *Pb*A-luc sporozoites. Patency was determined by microscopic enumeration of thin blood smears. Data are from two independent experiments, with 3-4 animals per group; p<0.0001 by Log-rank (Mantel Cox) test.

Figure 3. CD74 expression is essential for the development of ECM induced by *Pb*A infection. A, *Cd7*4 mRNA expression measured by qPCR in the brains of wild type (WT) C57BL6/J mice that were either non-infected (NI WT) or infected with 10^6 *Pb*A iRBC (INF WT). Results are shown as mean ± SD from two independent experiments with 6 animals per group and experiment: #p<0.0001 by Mann-Whitney test. CD74 deficient (*Cd74*$^{-/-}$) and WT C57BL6/J mice were infected i.p with 10^6 *Pb*A iRBC and the **B**, Kaplan–Meier survival plots for WT and *Cd74*$^{-/-}$ treated mice following infection with *Pb*A. Data are from two pooled independent experiments with 10 animals per group; p < 0.0001 by log-rank (Mantel Cox) test **C**, peripheral blood parasitemia. Data are shown as mean ± SD of n=10 WT and n=10 *Cd74*$^{-/-}$ mice and pooled from three independent experiments. **D**, Transcriptional expression of IFNγ, perforin and granzyme B was measured in brain tissue of *Pb*A infected WT and *Cd74*$^{-/-}$ mice on day 7 after infection by quantitative real-time PCR. Results are expressed as mean ± SD of n=6 mice per group pooled from two experiments: *p=0.0159 and *p=0.0317 by two-tailed Mann-Whitney test. Brain infiltrating lymphocytes from WT and *Cd74*$^{-/-}$ *Pb*A infected mice were isolated 7 days after infection, and the number of **E**, pathogenic tetramer-labeled brain CD8+ T cells (CD8$^+$GAP50Tetra^{hi}), and expressing **F**, the proinflammatory marker GrzmB (CD8$^+$GAP50Tetra^{hi}GrzmB^{hi}) measured by flow cytometry. Data are shown as mean ± SD of n=6 WT and n=6 *Cd74*$^{-/-}$ mice and pooled from two independent experiments; n.s.=non-significant; *p=0.0022 by two-tailed Mann-Whitney test. Cross-presentation of *Pb*AGAP$_{50}$ by brain endothelial cells. **G**, BEC isolated from WT and *Cd74*$^{-/-}$ mice were stimulated with 10 ng/ml IFNγ for 24 h, and then incubated for additional 24h with *Pb*A mature stage iRBCS before co-culture with LR-BSL8.4a reporter cells overnight prior to β-galactosidase activity assessment. Data are shown as mean ± SD of three independent biological replicates performed in triplicate; #p<0.0001 by Mann-Whitney test. **H**, Brain microvessel cross-presentation of

*Pb*AGAP$_{50}$ from naïve and *Pb*A infected WT and C*d74*$^{-/-}$ mice. Mice were infected with 10^6 *Pb*A, iRBC and brain microvessels were isolated when WT-infected mice exhibited neurological signs at 7 days after infection and co-incubated with LR-BSL8.4a reporter cells for 24 h and then assessed for β-galactosidase activity. Data are shown as mean ± SD of n=6 mice per group and pooled from two independent biological replicates; **p=0.0021 by Mann-Whitney test.

Figure 4. The small molecule PMIF antagonist 26k reduces *Pb*A infection in cultured hepatocytes and reduces PMIF/CD74 axis dependent survival. HepG2 cells ($1x10^5$ cells/well) were infected with $2x10^3$ *Pb*AWT sporozoites and treated with 26k or vehicle. **A**, Hepatocellular parasite load was measured by quantitative PCR of *Pb*A 18S rRNA relative to host GAPDH 48 h after treatment with 26k (0.5 nM to 50 μM) or vehicle. Data are from three independent experiments performed in duplicate. Bars represent the mean ± SD; *p=0.0336, **p=0.0021, Ψp=0.0008, #p<0.0001 by Kruskal-Wallis test. **B,** Percentage of apoptotic *Pb*AWT infected hepatocytes measured by AnnexinV and 7AAD staining after 26k or vehicle treatment. $1x10^5$ *Pb*AWT infected hepatocytes treated with 26K (100 nM) or vehicle were cultured for 48 h followed by the addition of the NO donor SNP (1 mM) for 4 h to induce apoptosis. Data are from three independent experiments performed in duplicate. Bars represent the mean ± SD; *p=0.0011; by two-tailed Mann-Whitney test. **C,** *Pb*AWT infected hepatocytes were lysed and assessed for total p53 and p53^{Ser15} by Western blotting with β-actin as loading control. Numerals represent the mean densitometric scanning ratios. Data are representative of two independent replicate experiments for the western blot analysis. NI: non-infected, INF: *Pb*A infected. C57BL/6J mice were treated with vehicle or 26k (80 mg/kg, ip) before (0 h), 24 h, and 48 h after i.v. infection with $2x10^3$ *Pb*A-luciferase sporozoites. **D,** Liver *Pb*A-luc burden was quantified by luminescence and **E,** by qPCR of liver *Pb*A 18S rRNA relative to host GAPDH 48 h after infection. Bars represent the mean ± SD; **p=0.0043 (**D**), **p=0.0079 (**E**); by Mann-Whitney test. **F**, Kaplan–Meier survival plots for vehicle and 26k treated mice following infection with *Pb*A-luc sporozoites. Data are from two pooled independent experiments with 6 animals per group; **p = 0.0023 by log-rank (Mantel Cox) test. **G**, Brain microvessel cross-presentation of *Pb*AGAP50 from vehicle and 26k treated mice following infection with PbA-luc sporozoites. Brains microvessels were isolated when vehicle-treated, infected mice exhibited neurological signs at 9 days after infection and co-incubated with LR-BSL8.4a reporter cells for 24 h and then assessed for β-galactosidase activity. Data are shown

as mean ± SD of n=6 mice per group and pooled from two independent biological replicates; **p=0.0022 by two-tailed Mann-Whitney test.

Supplementary Figures

Figure S1. PMIF promotes hepatocellular Akt phosphorylation, *Plasmodium* sporozoite infection of liver, and the survival of infected hepatocytes *in vivo*. **A**, Hepatocellular content of MSP-1 at 48 h after infection with 2x103 *Pb*AWT or *Pb*A*mif*- sporozoites assessed by western blot relative to PbHSP70 as loading control. Cultured hepatocytes ($1x10^5$ HepG2 cells/well) infected with $2x10^3$ *Pb*AWT or *Pb*A*mif*- sporozoites followed by the addition of 1 mM SNP at 4 h and 48 h after infection. B, Lysates were assessed for total Akt and $pAkt^{Ser473}$ by Western blotting with β-actin as loading control. Numerals represent the densitometric scanning ratios. **C**, C57BL/6J mice were with infected i.v. with $2x10^3$ *Pb*AWT or *Pb*A*mif*- sporozoites and hepatic parasite content measured by quantitative PCR of *Pb*A 18S rRNA relative to host GAPDH at 48 h after infection, bars represent the mean ± SD; **p=0.0050 by Mann-Whitney test. The expression of *Bcl-2* and *Bad* were measured by qPCR relative to *Pb*A18s 48 h after infection. Bars represent the mean ± SD; **p=0.0072 and *=0.0278 by Mann-Whitney test. The results are representative of 2 separate experiments (n=3 mice/group). **D**, Kaplan–Meier survival plots for C57BL6/J mice infected with $2x10^3$ *Pb*AWT or *Pb*A*mif*- sporozoites. Data are from two pooled independent experiments with a total of 6 animals per group; $p< 0.0001$ by log-rank (Mantel Cox) test. **F**, Kaplan-Meier survival plots for C57BL6/J mice infected with i.p with 10^6 PbAWT or PbAmif- iRBC. Data are form three pooled independent experiments with a total of 6 animals per group. n.s: non-significant by log-rank (Mantel Cox) test. **G**, Percentage of AnnexinV- cells among cultured hepatocytes ($1x10^5$ HepG2 cells) treated with 10 nM of shRNA directed at CD74 (shCD74) or a control shRNA (shCon) for 24h.

Figure S2. CD74 is essential for the development of ECM. Wild type (WT) and *Cd74* deficient (*Cd74*$^{-/-}$) C57BL6/J mice were infected i.p with 10^6 *Pb*A iRBC and **A,** ECM malaria score was assessed as described before and **B**, peripheral blood parasitemia was measured by flow cytometry. Bars represent the ± SD of n=10 WT and n=10 *Cd74*$^{-/-}$ mice and pooled from three independent experiments; n.s.=non-significant by Two-Way ANOVA. Wild type (WT) and *Cd74*$^{-/-}$ C57BL6/J mice were infected i.p with 10^6 *Pb*A*mif* iRBC **C**, Kaplan–Meier survival plots for WT and *Cd74*$^{-/-}$ mice following infection with *Pb*A*mif*. Data are from two pooled independent experiments with 10 animals per group; $p < 0.0001$ by log-rank (Mantel

Cox) test **D**, peripheral blood parasitemia. Data are shown as mean ± SD of n=7 WT and n=10 *Cd74*$^{-/-}$ mice and pooled from 2 independent experiments. **E**, ECM malaria score was assessed as described before. **F**, *Pb*A18s transcript expression in the brain of infected WT and *Cd74*$^{-/-}$ measured by quantitative real-time PCR 7 days after infection was measured in brains tissue of *Pb*A infected WT and *Cd74*$^{-/-}$ mice on day 7 after infection by quantitative real-time PCR. Results are expressed as mean ± SD of n=6 mice per group pooled from two experiments; n.s.: non-significant by Mann-Withney test. WT C57BL6/J mice were infected i.v with $2x10^3$ *Pb*AWT or *Pb*A*mif-* sporozoites. **G,** CD74 transcript expression in the brain of infected mice was measured by q-PCR at day 8 after infection. Results are expressed as mean ± SD of n=6 mice per group pooled from two experiments; **p=0.0022 by Mann-Whitney test. **H**, Transcriptional expression of IFNγ, Perforin and Granzyme B was measured in brain tissue of *Pb*AWT or *Pb*A*mif-* infected WT mice on day 8 after infection by quantitative real-time PCR. Results are expressed as mean ± SD of n=6 mice per group pooled from two experiments; **p=0.0022 for Perforin and IFNγ and **p=0.0317 for Granzyme B, by two-tailed Mann-Whitney test. **I**, Brain microvessel cross-presentation of *Pb*AGAP50 from naïve (NI) and *Pb*AWT or *Pb*A*mif* infected WT mice. Mice were infected with *Pb*AWT or *Pb*A*mif-* sporozoites and brain microvessels were isolated when *Pb*AWT-infected mice exhibited neurological signs at 7 days after infection. Microvessels then were co-incubated with LR-BSL8.4a reporter cells for 24 h and then assessed for β-galactosidase activity. Data are shown as mean ± SD of n=6 mice per group and pooled from two independent biological replicates; **p=0.0021 by Mann-Whitney test. **J**, Brain microvessel cross-presentation of *Pb*AGAP50 from *Cd8*$^{-/-}$ and *Cd8*$^{-/-}$*Cd74*$^{-/-}$ receiving CD8$^+$ T cells isolated from *Pb*A infected WT or *Cd74*$^{-/-}$ mice three days before the infection with 10^6 *Pb*AWT iRBC. Brain microvessels were isolated when the first infected mice exhibited neurological signs at 7 days after infection and co-incubated with LR-BSL8.4a reporter cells for 24 h and then assessed for β-galactosidase activity. Data are shown as mean ± SD of n=5 mice per group and pooled from two independent biological replicates; # p=0.0017 and **p<0.0001 by Kruskal-Wallis test. **K**, Kaplan-Meier survival plots for C57BL6/J mice *Cd8*$^{-/-}$ and *Cd8*$^{-/-}$*Cd74*$^{-/-}$ receiving CD8$^+$ T cells isolated from *Pb*A infected WT or *Cd74*$^{-/-}$ and infected with i.p with 10^6 *Pb*AWT iRBC. Data are form three pooled independent experiments with 6 animals per group; p<0.0001 by log-rank (Mantel Cox) test. **L.** Effect of human serum on PMIF binding to the immobilized human CD74 ectodomain (aa 134-232). Measured values are relative to control without serum for each condition (n=6 healthy uninfected controls, n=6 uncomplicated malaria, n=6 complicated malaria. Mean±SD; #p<0.0001 by 1-way ANOVA.

Figure S3. The small molecule PMIF antagonist 26k reduces PMIF/CD74 signal transduction and protects from ECM. A. BMDM were treated with or without recombinant PMIF pre-incubated with vehicle control (DMSO) or small molecule 26k (10,50 or 100 nM) for 2h. Cells were lysed and the lysates assessed for total ERK and pERK$^{Thr202/Tyr204}$ by western blotting. C57BL/6J mice were treated with vehicle or 26k (80 mg/kg, ip) before (0 h), 24 h, and 48 h after i.v. infection with 2x10^3 *Pb*A-luciferase sporozoites. Numerals represent the densitometric scanning ratios. **B,** Kaplan-Meier plots showing the percentage of vehicle (o) and 26k (●) treated mice with blood-stage patency following i.v. infection with 2x10^3 *Pb*A-luc sporozoites. Patency was determined by microscopic enumeration of thin blood smears. Data are from two pooled independent experiments, with 6 animals per group; $p<0.0001$ by Log-rank (Mantel Cox) test. **C**, Kaplan–Meier survival plots for vehicle (o) and 26k (●) treated mice following infection with *Pb*A iRBC. Data are from two pooled independent experiments with 8 animals per group; $p = 0.0137$ by log-rank (Mantel Cox) test

Figure S4. Suppression of *Plasmodium* MIF-CD74 Signaling Protects Against Severe Malaria. After the bite of infected *Anopheles* mosquitoes, *Plasmodium* sporozoites transit through the bloodstream to invade the liver. (**1)** PMIF through the interaction with its host receptor CD74 promotes *Plasmodium*-infected hepatocyte survival via p53 inhibition. This results in blood-stream emergence and erythrocyte infection. Circulating iRBCs bind to brain endothelium initiating activation and promoting parasite adhesion and accumulation. PMIF binds with CD74, and increases CD74 transcription and cross-presentation of *Plasmodium* antigens by endothelial cells to sequestered CD8+ T cells that produce inflammatory molecules including Granzyme B, Perforin and IFNγ, leading to Blood Brain Barrier (BBB) breakdown and leakage. The absence of PMIF (**2**) or inhibition of PMIF binding to the CD74 ectodomain by the small molecule PMIF antagonist 26k (**3**) promotes *Plasmodium*-infected hepatocyte apoptosis and p53 activation. This results in a delayed blood patency. Circulating iRBCs still bind to brain endothelium receptors, initiating endothelial cell activation and parasite adhesion and accumulation. Nevertheless, inhibition or absence of binding between PMIF and CD74 decreases cross-presentation of *Pb*A antigens by endothelial cells to CD8+T cells and results in reduced Granzyme B, Perforin and IFNγ production and protection of BBB integrity.

References

1. WHO. World malaria report 2019. 2019.
2. van de Sand C, Horstmann S, Schmidt A, Sturm A, Bolte S, Krueger A, et al. The liver stage of Plasmodium berghei inhibits host cell apoptosis. Molecular Microbiology. 2005;58(3):731-42. doi: 10.1111/j.1365-2958.2005.04888.x.
3. Leirião P, Albuquerque SS, Corso S, Van Gemert G-J, Sauerwein RW, Rodriguez A, et al. HGF/MET signalling protects Plasmodium-infected host cells from apoptosis. Cellular Microbiology. 2005;7(4):603-9. doi: 10.1111/j.1462-5822.2004.00490.x.
4. Kaushansky A, Ye Albert S, Austin Laura S, Mikolajczak Sebastian A, Vaughan Ashley M, Camargo N, et al. Suppression of Host p53 Is Critical for Plasmodium Liver-Stage Infection. Cell Reports. 2013;3(3):630-7. doi: http://doi.org/10.1016/j.celrep.2013.02.010.
5. Langhorne J, Ndungu FM, Sponaas A-M, Marsh K. Immunity to malaria: more questions than answers. Nature Immunology. 2008;9:725. doi: 10.1038/ni.f.205.
6. Milner DA, Whitten RO, Kamiza S, Carr R, Liomba G, Dzamalala C, et al. The systemic pathology of cerebral malaria in African children. Frontiers in Cellular and Infection Microbiology. 2014;4(104). doi: 10.3389/fcimb.2014.00104.
7. Shaw TN, Stewart-Hutchinson PJ, Strangward P, Dandamudi DB, Coles JA, Villegas-Mendez A, et al. Perivascular Arrest of CD8+ T Cells Is a Signature of Experimental Cerebral Malaria. PLOS Pathogens. 2015;11(11):e1005210. doi: 10.1371/journal.ppat.1005210.
8. Howland SW, Poh CM, Rénia L. Activated Brain Endothelial Cells Cross-Present Malaria Antigen. PLOS Pathogens. 2015;11(6):e1004963. doi: 10.1371/journal.ppat.1004963.
9. Aurrecoechea C, Brestelli J, Brunk BP, Dommer J, Fischer S, Gajria B, et al. PlasmoDB: a functional genomic database for malaria parasites. Nucleic Acids Research. 2008;37(suppl_1):D539-D43. doi: 10.1093/nar/gkn814.
10. Aurrecoechea C, Barreto A, Basenko EY, Brestelli J, Brunk BP, Cade S, et al. EuPathDB: the eukaryotic pathogen genomics database resource. Nucleic Acids Research. 2016;45(D1):D581-D91. doi: 10.1093/nar/gkw1105.
11. Mitchell RA, Liao H, Chesney J, Fingerle-Rowson G, Baugh J, David J, et al. Macrophage migration inhibitory factor (MIF) sustains macrophage proinflammatory function by inhibiting p53: Regulatory role in the innate immune response. Proceedings of the National Academy of Sciences. 2002;99(1):345-50. doi: 10.1073/pnas.012511599.
12. Leng L, Metz CN, Fang Y, Xu J, Donnelly S, Baugh J, et al. MIF Signal Transduction Initiated by Binding to CD74. The Journal of Experimental Medicine. 2003;197(11):1467-76. doi: 10.1084/jem.20030286.
13. Kamir D, Zierow S, Leng L, Cho Y, Diaz Y, Griffith J, et al. A Leishmania Ortholog of Macrophage Migration Inhibitory Factor Modulates Host Macrophage Responses. The Journal of Immunology. 2008;180(12):8250-61. doi: 10.4049/jimmunol.180.12.8250.
14. Miller JL, Harupa A, Kappe SHI, Mikolajczak SA. Plasmodium yoelii Macrophage Migration Inhibitory Factor Is Necessary for Efficient Liver-Stage Development. Infection and Immunity. 2012;80(4):1399-407. doi: 10.1128/iai.05861-11.
15. Baeza Garcia A, Siu E, Sun T, Exler V, Brito L, Hekele A, et al. Neutralization of the Plasmodium-encoded MIF ortholog confers protective immunity against malaria infection. Nature Communications. 2018;9(1):2714. doi: 10.1038/s41467-018-05041-7.
16. Augustijn KD, Kleemann R, Thompson J, Kooistra T, Crawford CE, Reece SE, et al. Functional Characterization of the Plasmodium falciparum and P. berghei Homologues of Macrophage Migration Inhibitory Factor. Infection and Immunity. 2007;75(3):1116-28. doi: 10.1128/iai.00902-06.

17. Sun T, Holowka T, Song Y, Zierow S, Leng L, Chen Y, et al. A Plasmodium-encoded cytokine suppresses T-cell immunity during malaria. Proceedings of the National Academy of Sciences. 2012;109(31):E2117–E26. doi: 10.1073/pnas.1206573109.
18. Kaushansky A, Austin LS, Mikolajczak SA, Lo FY, Miller JL, Douglass AN, et al. Susceptibility to Plasmodium yoelii Preerythrocytic Infection in BALB/c Substrains Is Determined at the Point of Hepatocyte Invasion. Infection and Immunity. 2015;83(1):39-47. doi: 10.1128/iai.02230-14.
19. Prudêncio M, Mota MM, Mendes AM. A toolbox to study liver stage malaria. Trends in Parasitology. 2011;27(12):565-74. doi: 10.1016/j.pt.2011.09.004.
20. Lue H, Thiele M, Franz J, Dahl E, Speckgens S, Leng L, et al. Macrophage migration inhibitory factor (MIF) promotes cell survival by activation of the Akt pathway and role for CSN5/JAB1 in the control of autocrine MIF activity. Oncogene. 2007;26(35):5046-59.
21. Shao D, Zhong X, Zhou Y-F, Han Z, Lin Y, Wang Z, et al. Structural and functional comparison of MIF ortholog from Plasmodium yoelii with MIF from its rodent host. Molecular Immunology. 2010;47(4):726-37. doi: https://doi.org/10.1016/j.molimm.2009.10.037.
22. Howland SW, Claser C, Poh CM, Gun SY, Rénia L. Pathogenic CD8+ T cells in experimental cerebral malaria. Seminars in Immunopathology. 2015;37(3):221-31. doi: 10.1007/s00281-015-0476-6.
23. Howland SW, Poh CM, Gun SY, Claser C, Malleret B, Shastri N, et al. Brain microvessel cross-presentation is a hallmark of experimental cerebral malaria. EMBO Molecular Medicine. 2013;5(7):984-99. doi: 10.1002/emmm.201202273.
24. Cresswell P. Assembly, Transport, and Function of MHC Class II Molecules. Annual Review of Immunology. 1994;12(1):259-91. doi: 10.1146/annurev.iy.12.040194.001355. PubMed PMID: 8011283.
25. Basha G, Omilusik K, Chavez-Steenbock A, Reinicke AT, Lack N, Choi KB, et al. A CD74-dependent MHC class I endolysosomal cross-presentation pathway. Nature Immunology. 2012;13:237. doi: 10.1038/ni.2225
https://www.nature.com/articles/ni.2225#supplementary-information.
26. Han C, Lin Y, Shan G, Zhang Z, Sun X, Wang Z, et al. Plasma concentration of malaria parasite-derived macrophage migration inhibitory factor in uncomplicated malaria patients correlates with parasitemia and disease severity. Clin Vaccine Immunol. 2010;17(10):1524-32. Epub 08/11. doi: 10.1128/CVI.00149-10. PubMed PMID: 20702656.
27. Cournia Z, Leng L, Gandavadi S, Du X, Bucala R, Jorgensen WL. Discovery of human macrophage migration inhibitory factor (MIF)-CD74 antagonists via virtual screening. J Med Chem. 2009;52(2):416-24. Epub 2008/12/19. doi: 10.1021/jm801100v. PubMed PMID: 19090668; PubMed Central PMCID: PMCPMC2680181.
28. Pantouris G, Rajasekaran D, Garcia AB, Ruiz VG, Leng L, Jorgensen WL, et al. Crystallographic and Receptor Binding Characterization of Plasmodium falciparum Macrophage Migration Inhibitory Factor Complexed to Two Potent Inhibitors. Journal of Medicinal Chemistry. 2014;57(20):8652-6. doi: 10.1021/jm501168q.
29. Cho Y, Crichlow GV, Vermeire JJ, Leng L, Du X, Hodsdon ME, et al. Allosteric inhibition of macrophage migration inhibitory factor revealed by ibudilast. Proc Natl Acad Sci USA. 2010;107(25):11313-8.
30. Fox RJ, Coffey CS, Cudkowicz ME, Gleason T, Goodman A, Klawiter EC, et al. Design, rationale, and baseline characteristics of the randomized double-blind phase II clinical trial of ibudilast in progressive multiple sclerosis. Contemp Clin Trials. 2016;50:166-77. doi: 10.1016/j.cct.2016.08.009. PubMed PMID: 27521810; PubMed Central PMCID: PMCPMC5035622.
31. Dahlgren MK, Garcia AB, Hare AA, Tirado-Rives J, Leng L, Bucala R, et al. Virtual Screening and Optimization Yield Low-Nanomolar Inhibitors of the Tautomerase Activity of

755 Plasmodium falciparum Macrophage Migration Inhibitory Factor. Journal of Medicinal
756 Chemistry. 2012;55(22):10148-59. doi: 10.1021/jm301269s.
757 32. Lopes da Silva M, Thieleke-Matos C, Cabrita-Santos L, Ramalho JS, Wavre-Shapton
758 ST, Futter CE, et al. The host endocytic pathway is essential for Plasmodium berghei late liver
759 stage development. Traffic (Copenhagen, Denmark). 2012;13(10):1351-63. Epub 2012/07/12.
760 doi: 10.1111/j.1600-0854.2012.01398.x. PubMed PMID: 22780869.
761 33. Tanese K, Hashimoto Y, Berkova Z, Wang Y, Samaniego F, Lee JE, et al. Cell Surface
762 CD74-MIF Interactions Drive Melanoma Survival in Response to Interferon-γ. The Journal of
763 investigative dermatology. 2015;135(11):2775-84. Epub 2015/06/04. doi:
764 10.1038/jid.2015.204. PubMed PMID: 26039541; PubMed Central PMCID:
765 PMCPMC4640965.
766 34. Villegas-Mendez A, Strangward P, Shaw TN, Rajkovic I, Tosevski V, Forman R, et al.
767 Gamma Interferon Mediates Experimental Cerebral Malaria by Signaling within Both the
768 Hematopoietic and Nonhematopoietic Compartments. Infection and immunity.
769 2017;85(11):e01035-16. doi: 10.1128/IAI.01035-16. PubMed PMID: 28874445.
770 35. Fernandez-Ruiz D, Lau LS, Ghazanfari N, Jones CM, Ng WY, Davey GM, et al.
771 Development of a Novel CD4(+) TCR Transgenic Line That Reveals a Dominant Role for
772 CD8(+) Dendritic Cells and CD40 Signaling in the Generation of Helper and CTL Responses
773 to Blood-Stage Malaria. Journal of immunology (Baltimore, Md : 1950). 2017;199(12):4165-
774 79. Epub 2017/11/01. doi: 10.4049/jimmunol.1700186. PubMed PMID: 29084838; PubMed
775 Central PMCID: PMCPMC5713497.
776 36. Thuma PE, van Dijk J, Bucala R, Debebe Z, Nekhai S, Kuddo T, et al. Distinct clinical
777 and immunologic profiles in severe malarial anemia and cerebral malaria in Zambia. The
778 Journal of infectious diseases. 2011;203(2):211-9. Epub 2011/02/04. doi:
779 10.1093/infdis/jiq041. PubMed PMID: 21288821; PubMed Central PMCID:
780 PMCPMC3071068.

781

Fig 1

A

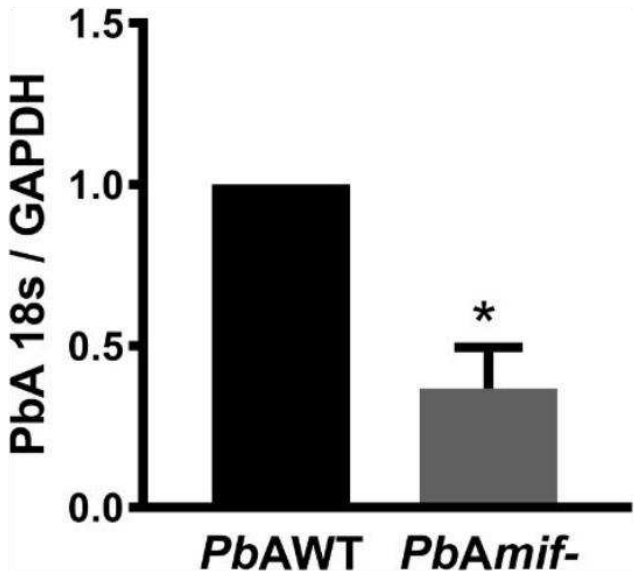

B

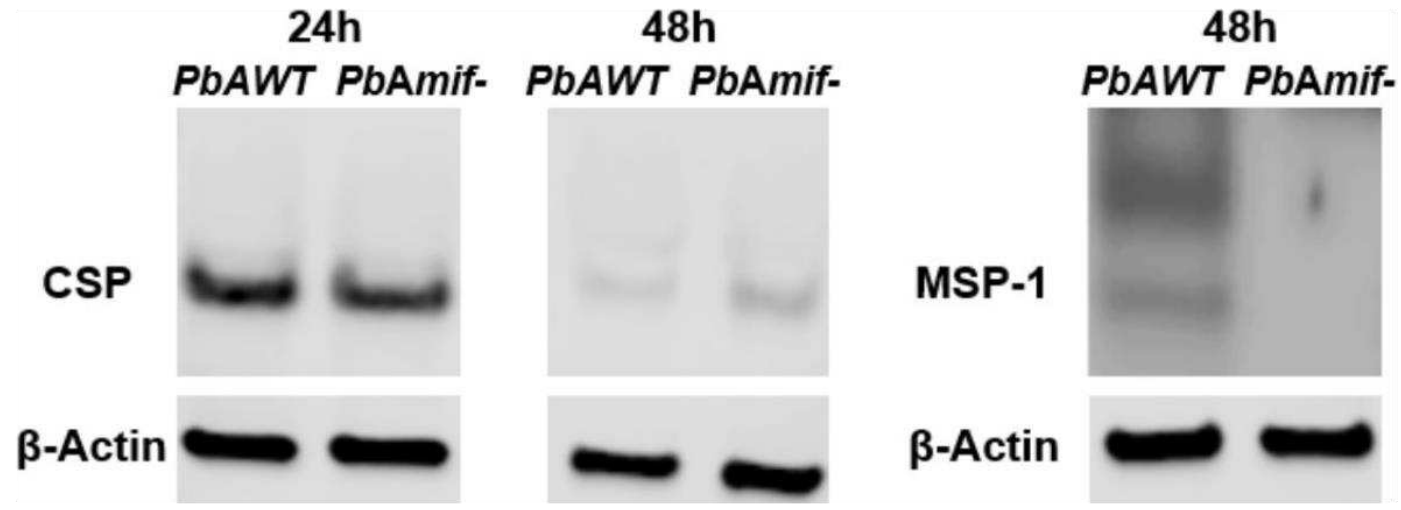

C

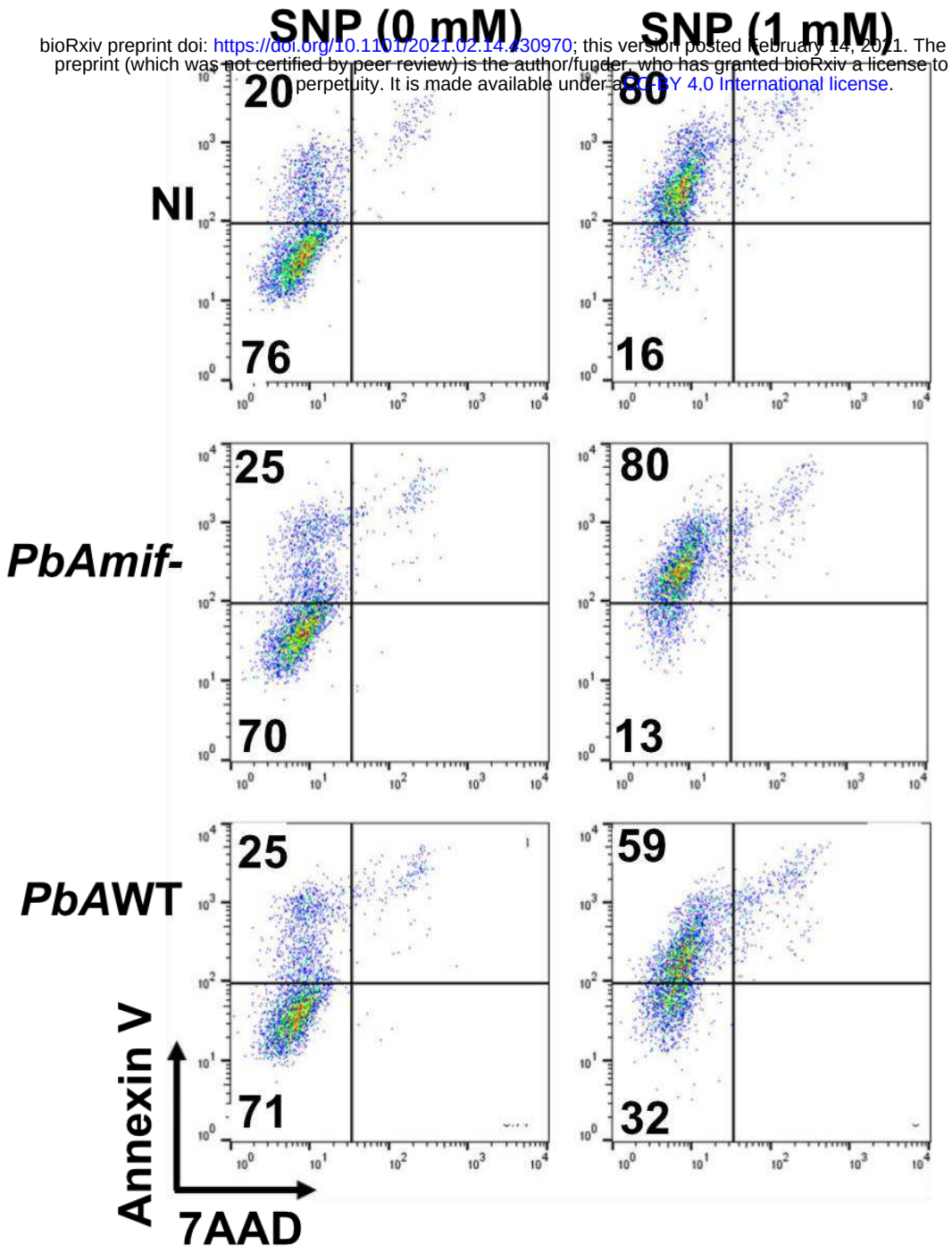

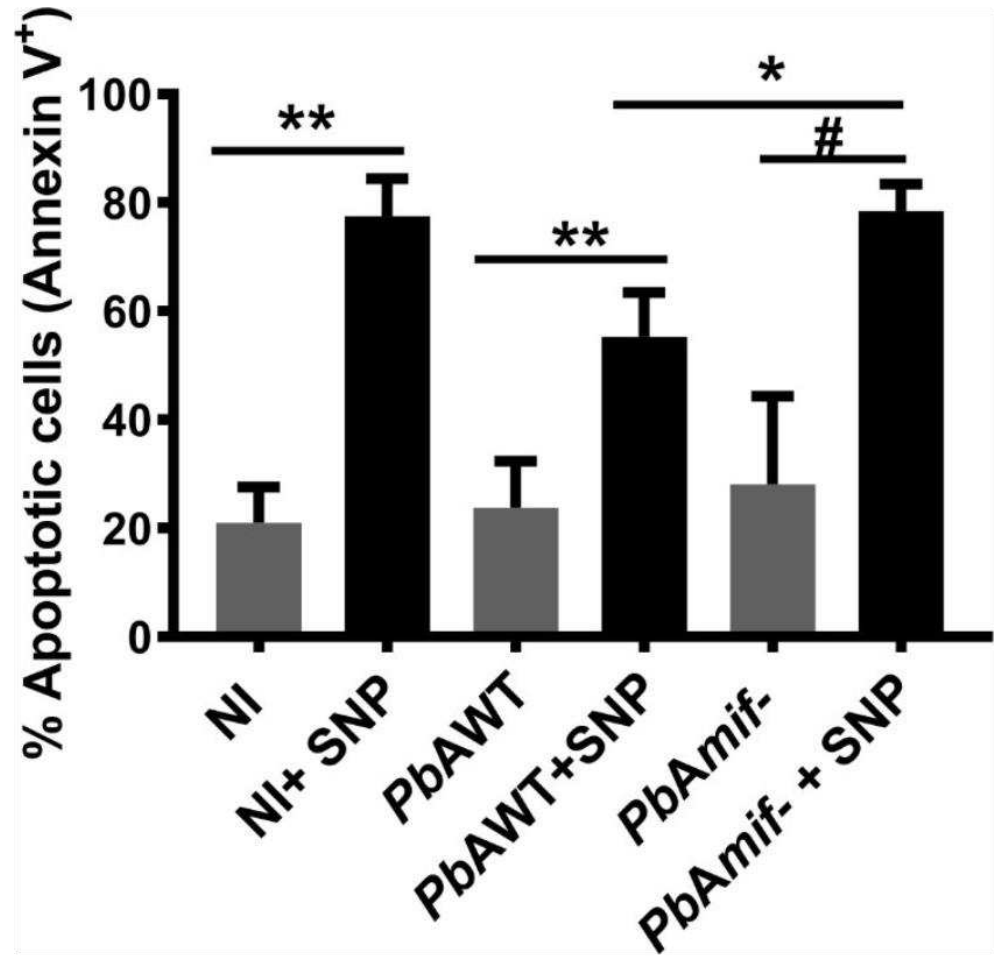

D

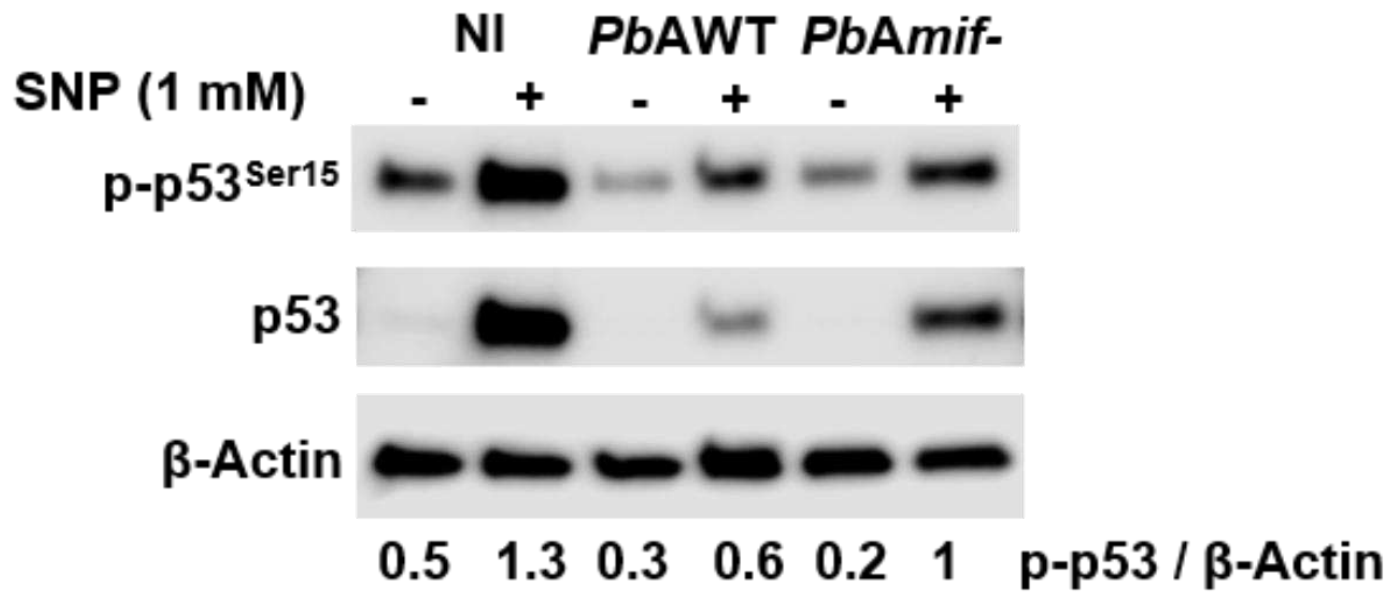

Fig 2

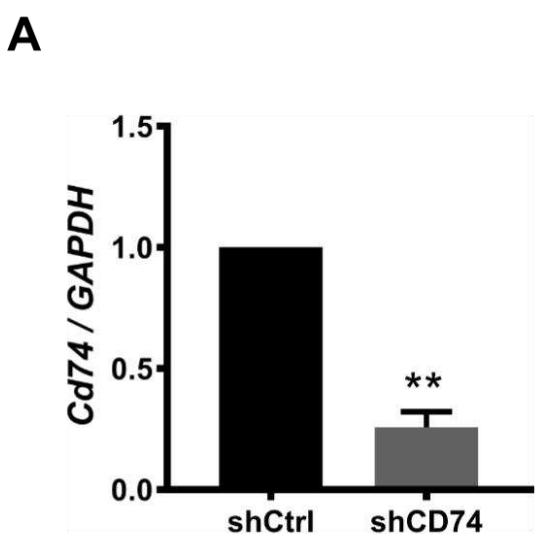

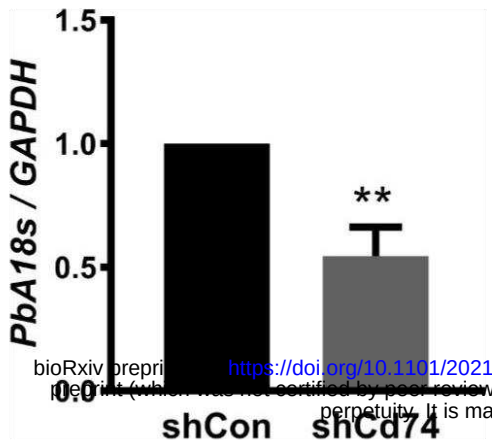

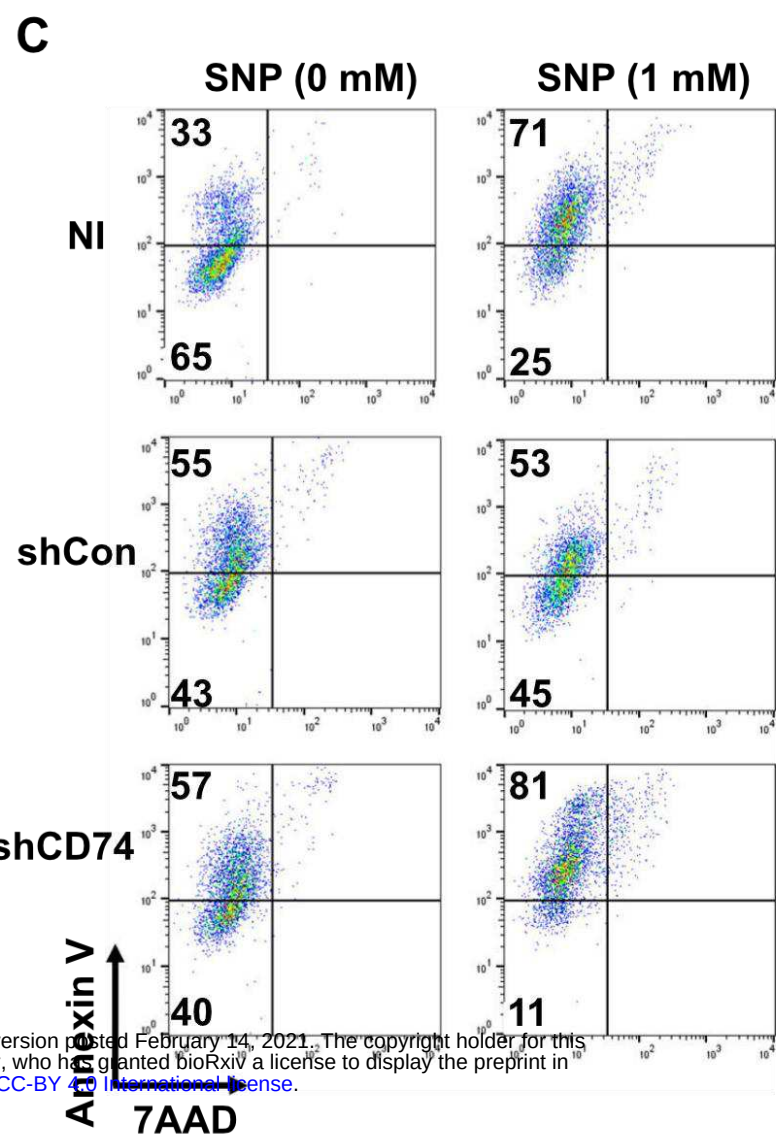

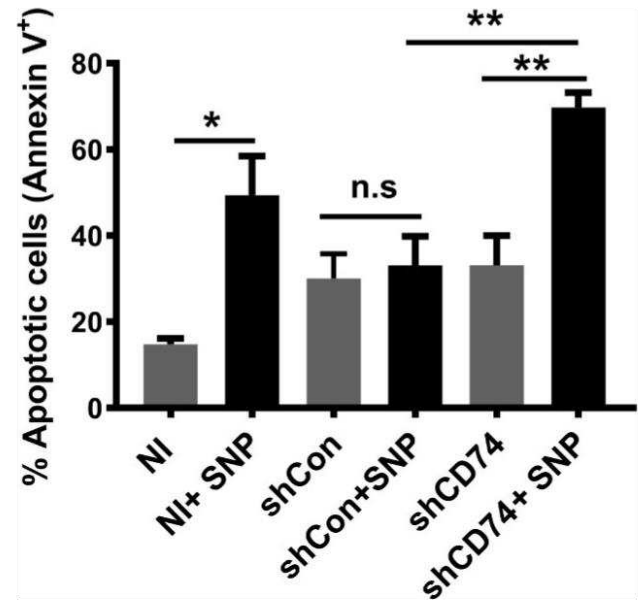

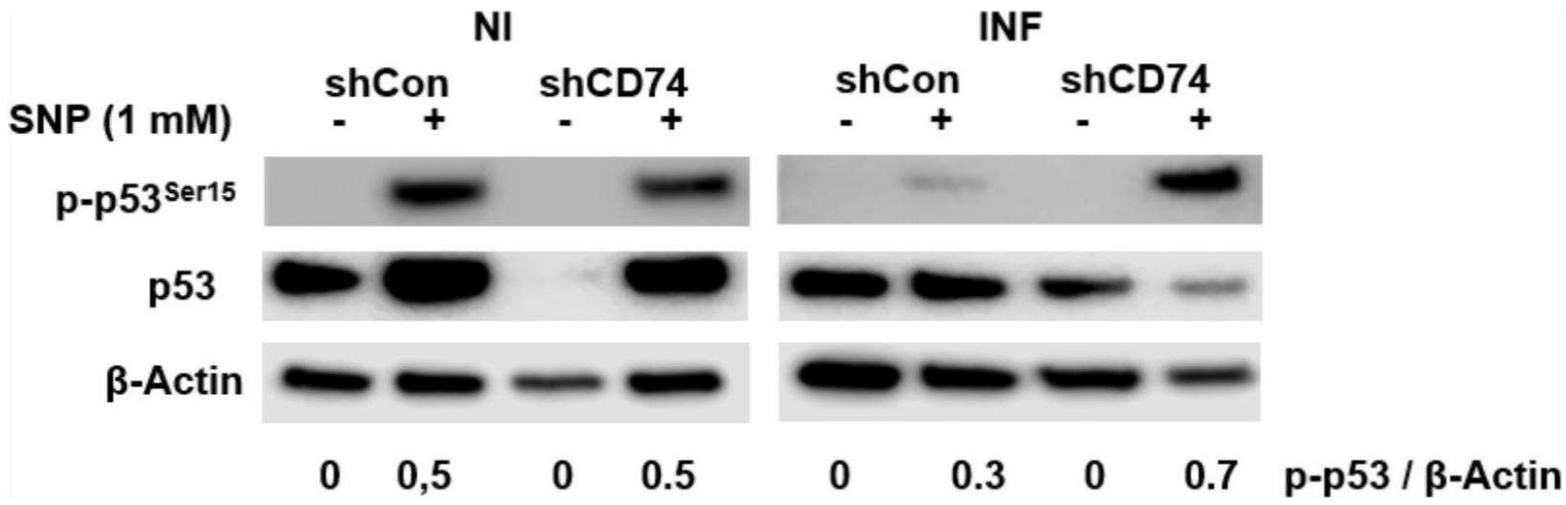

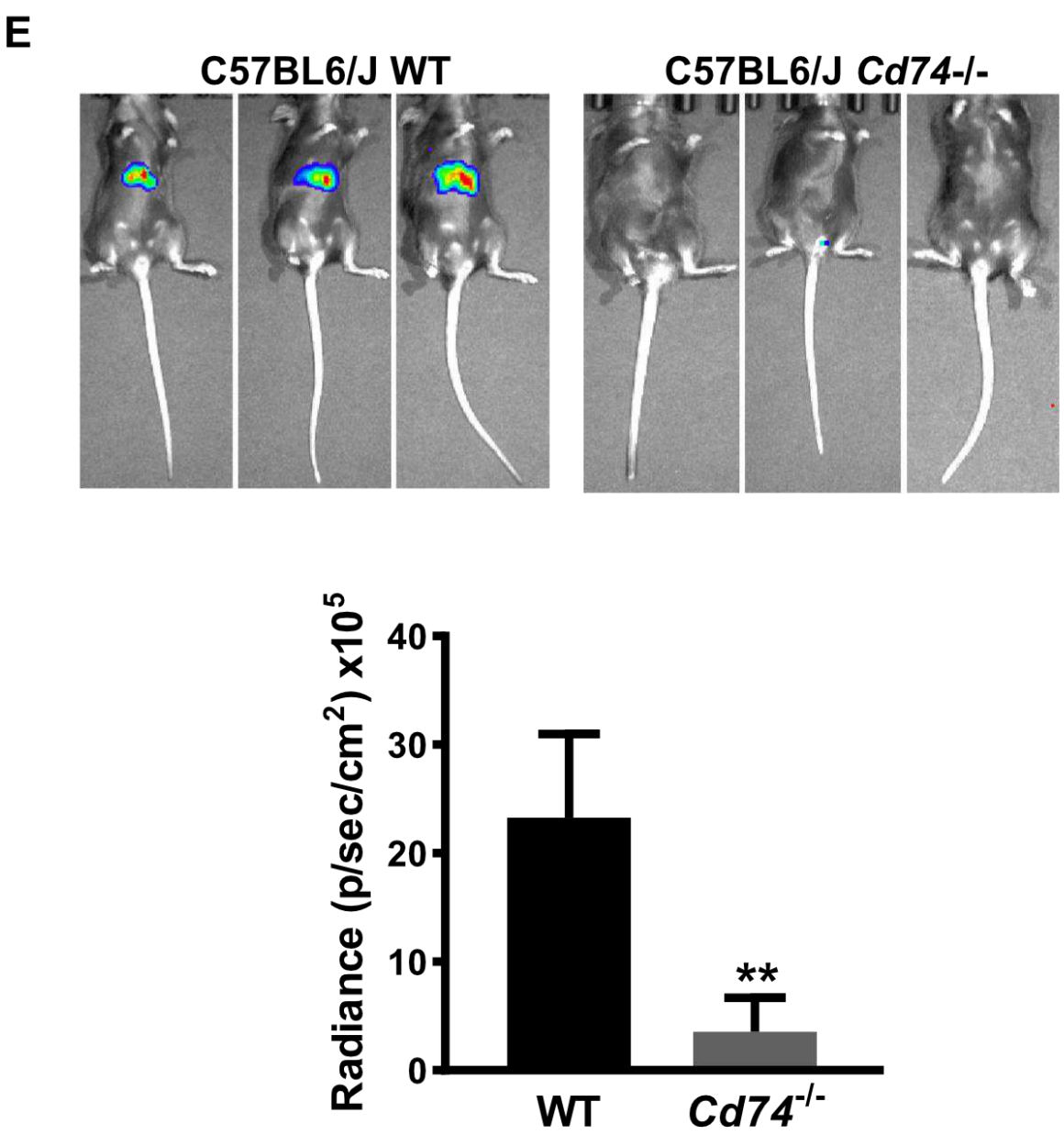

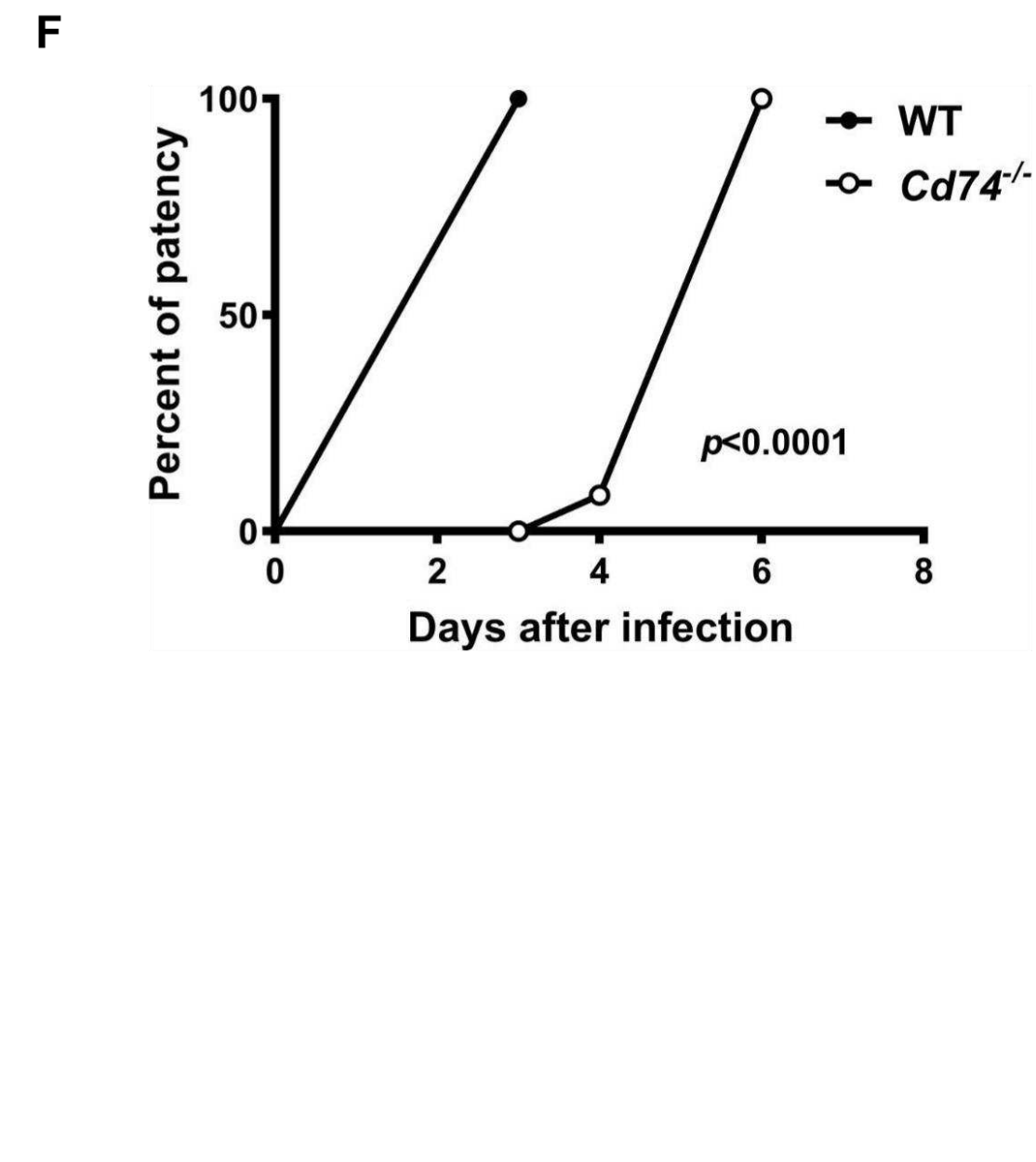

Fig 3

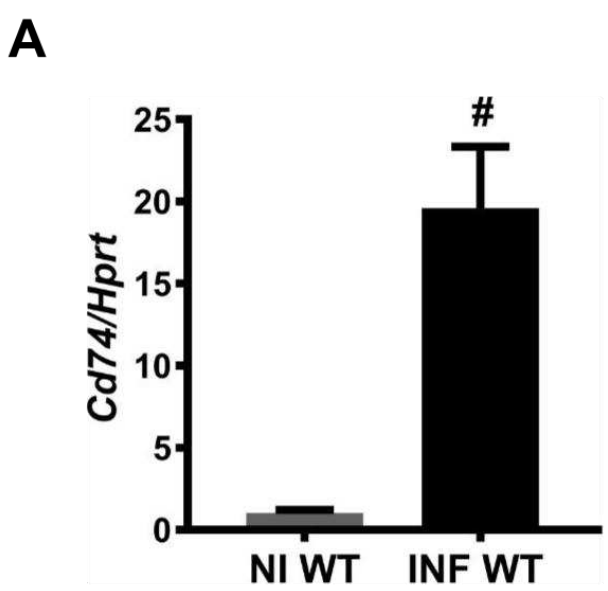

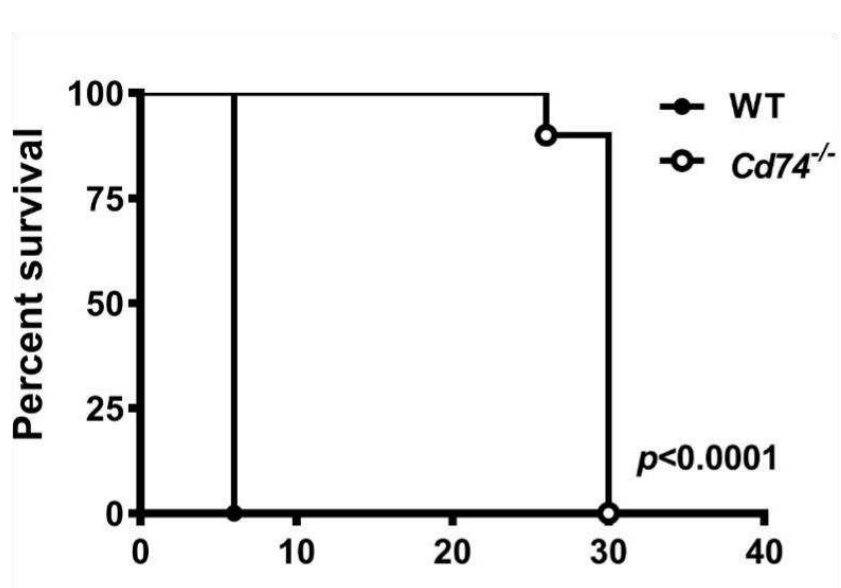

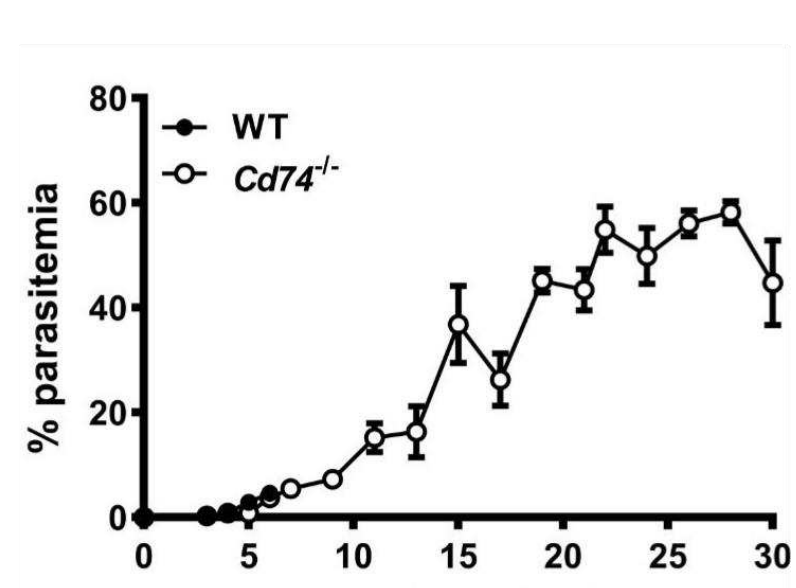

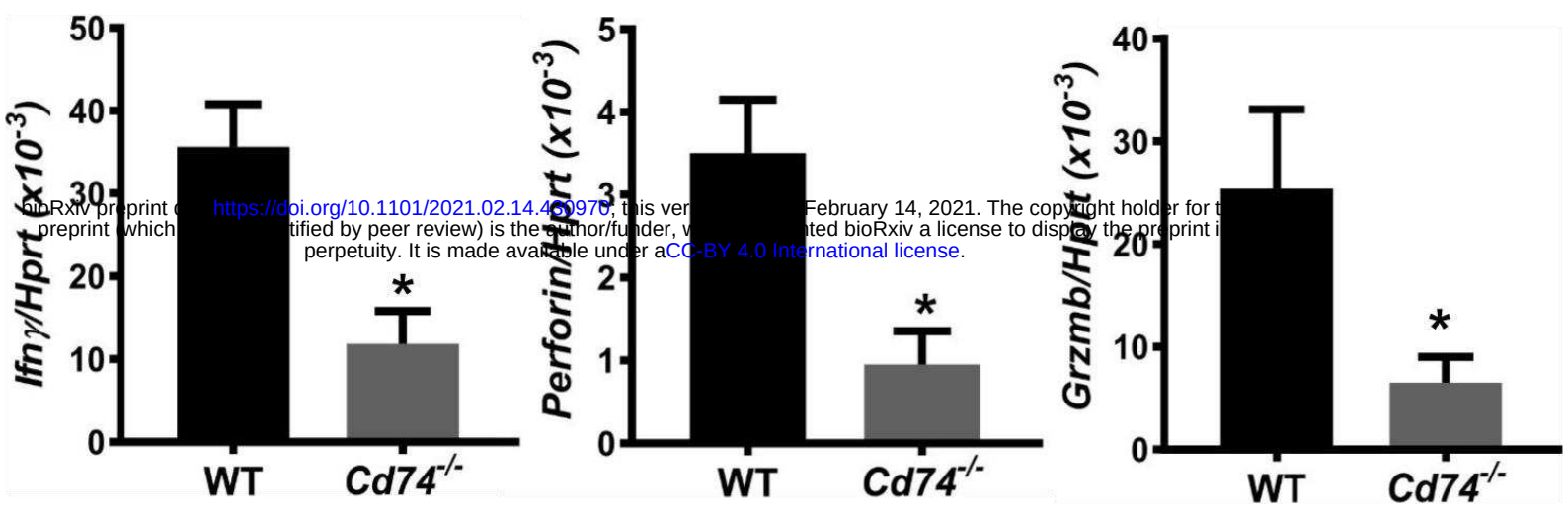

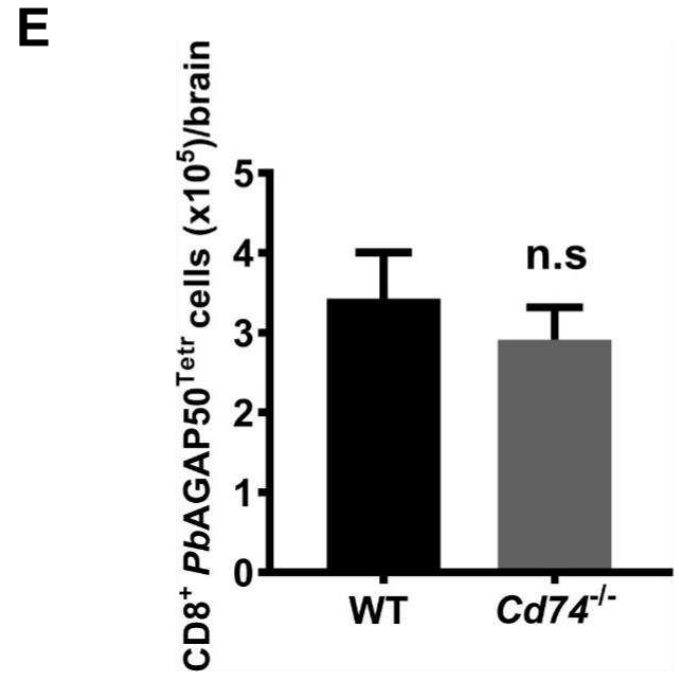

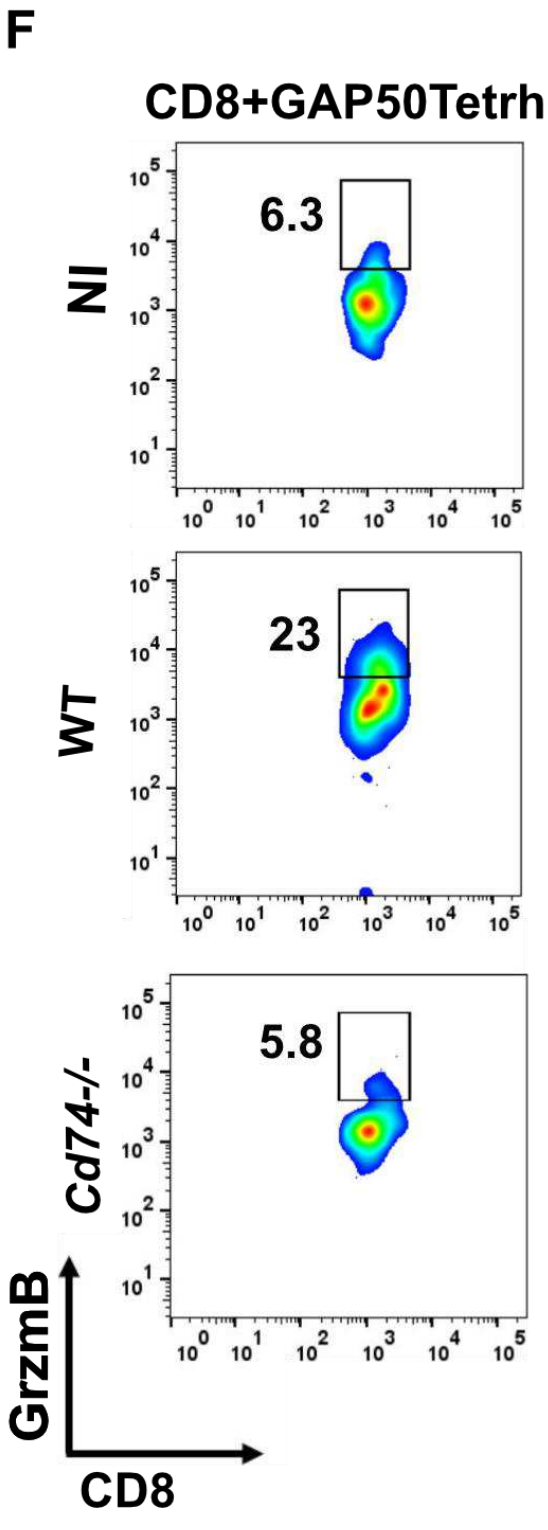

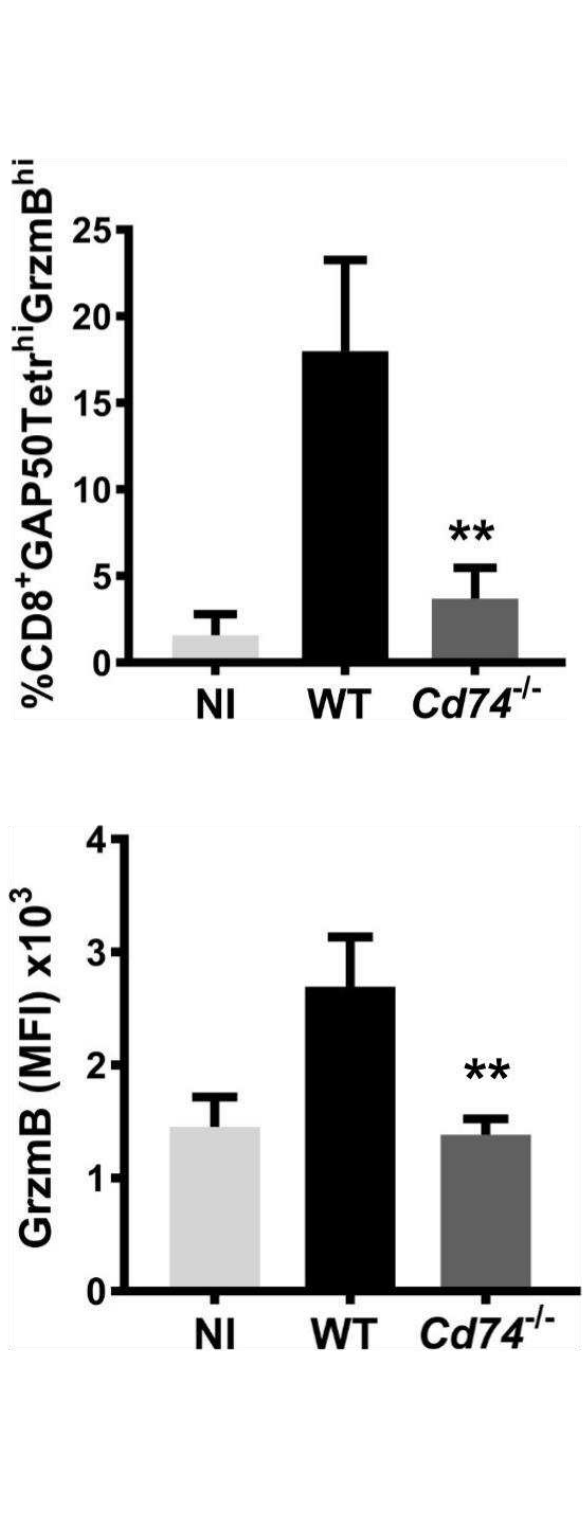

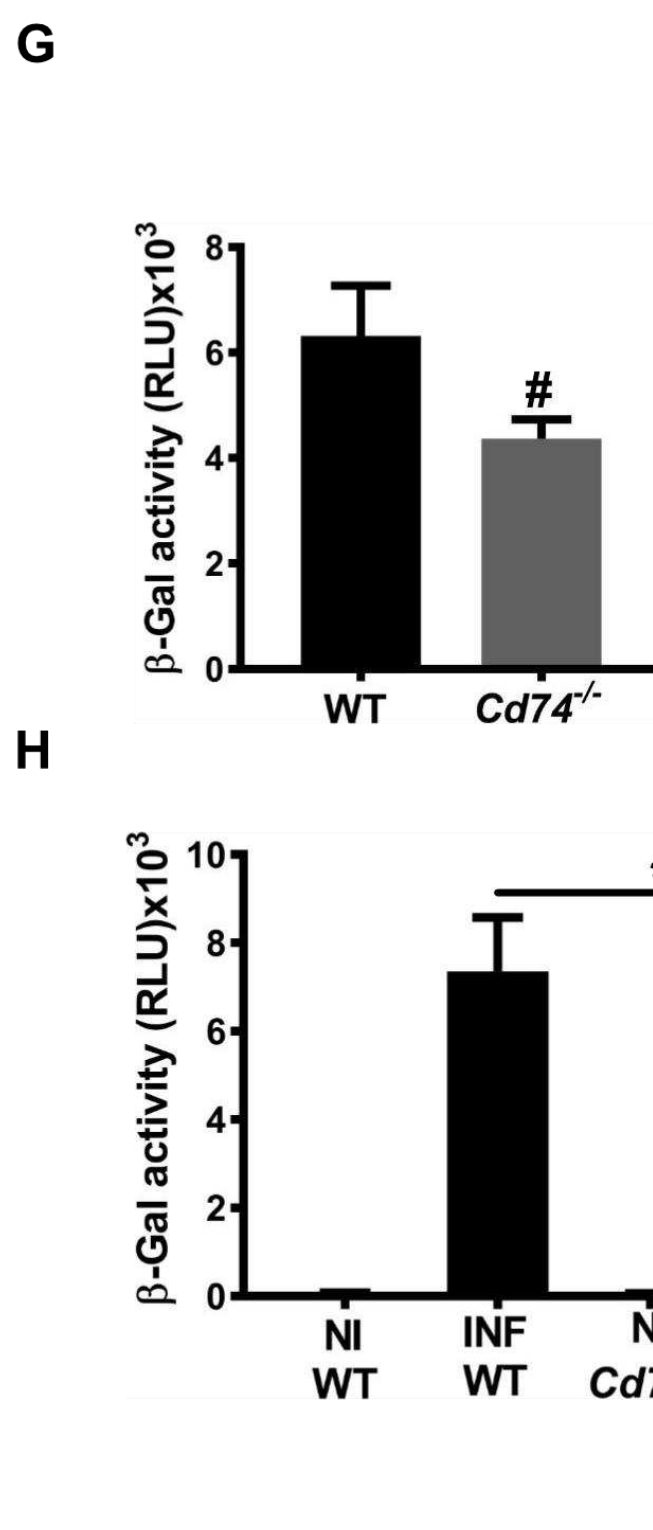

Fig 4

Figure S1

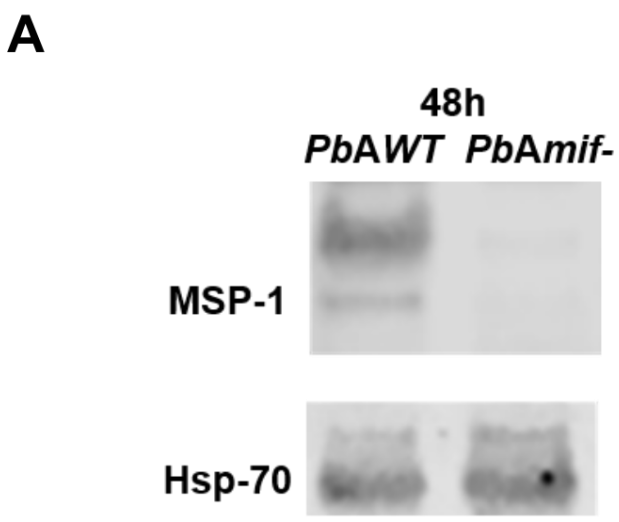

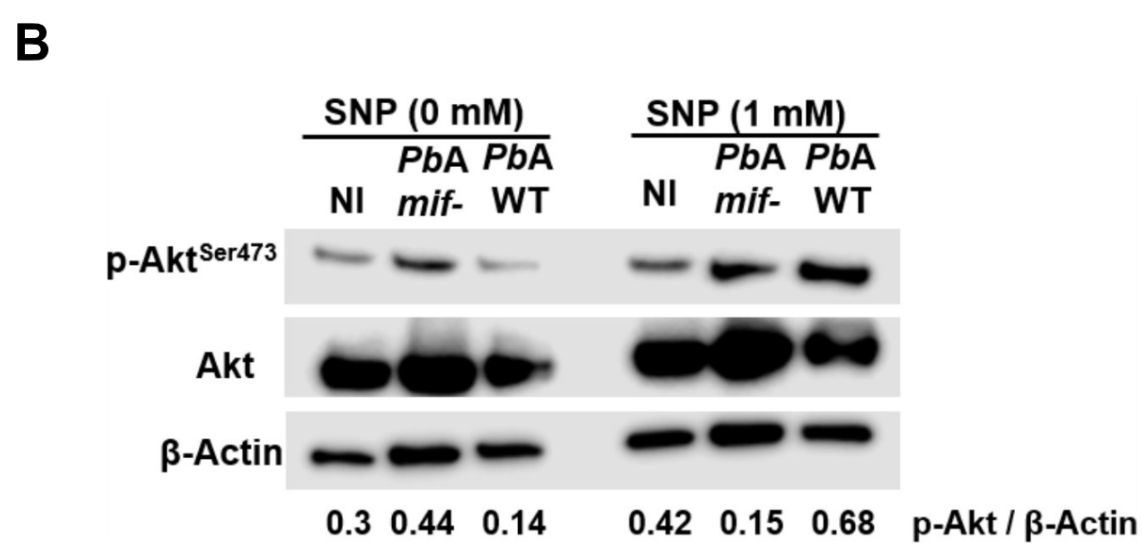

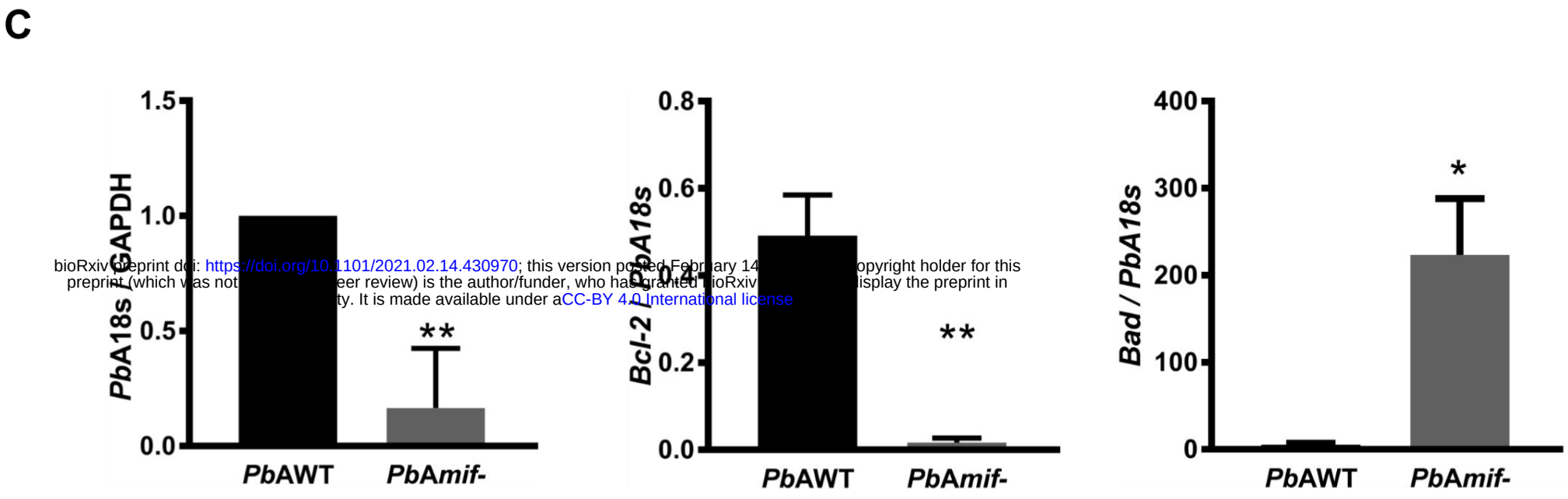

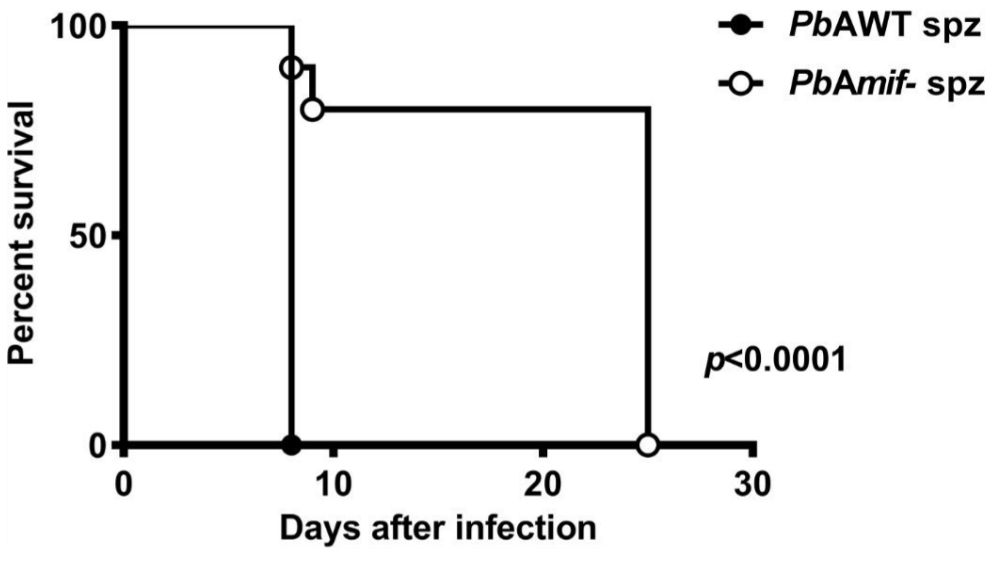

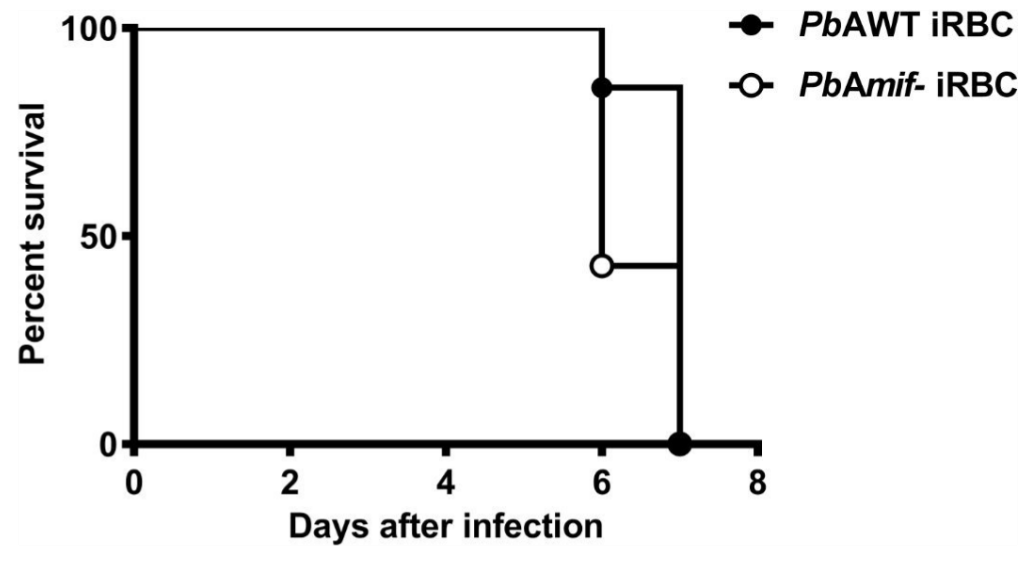

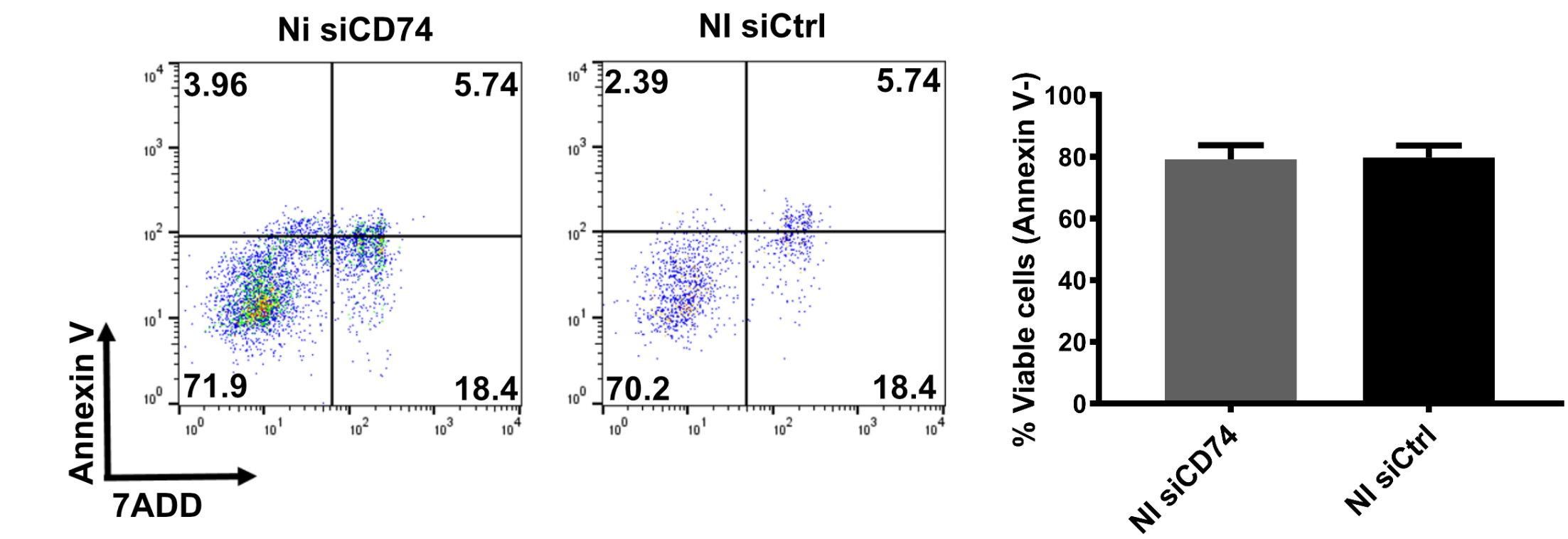

Figure S2

Figure S3

A

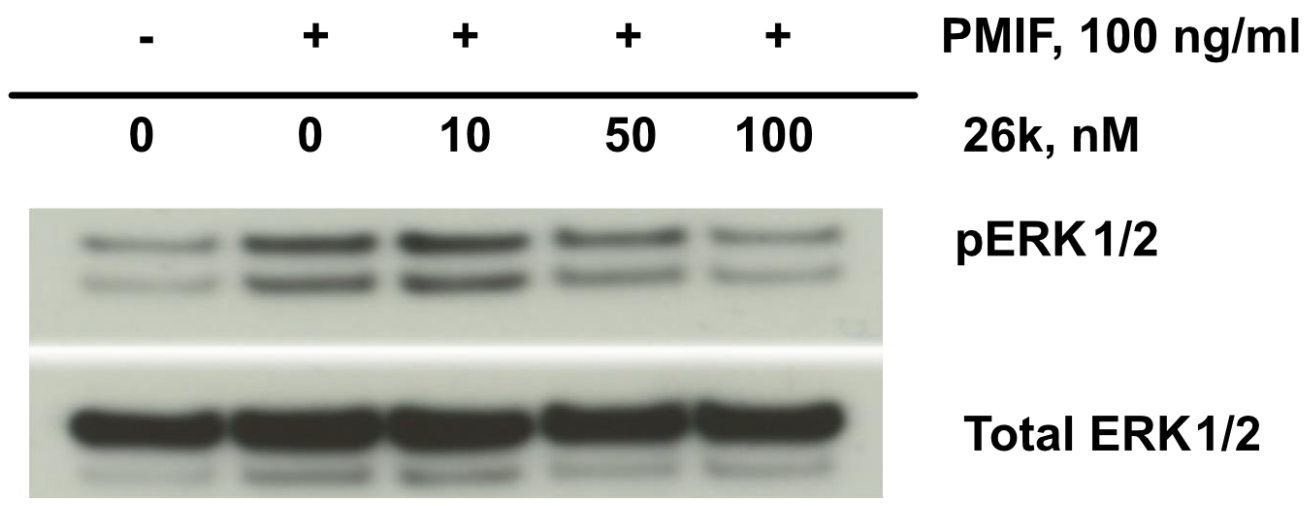

B

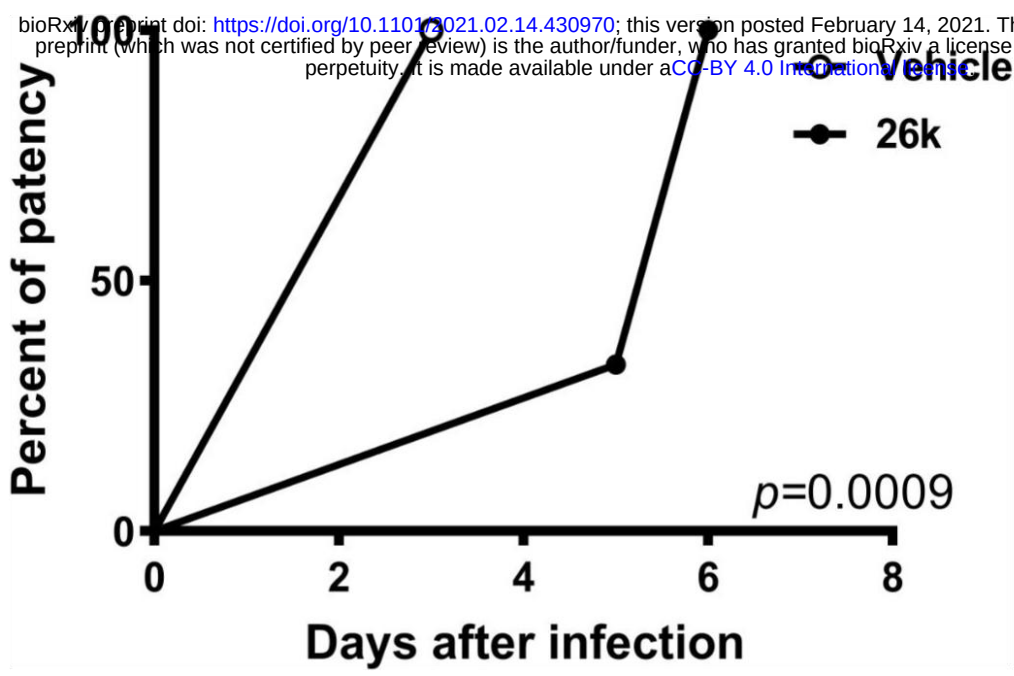

C